Available online at www.sciencedirect.com
ScienceDirect
Ore Geology Reviews 29 (2006) 260–286
ORE GEOLOGY REVIEWS
www.elsevier.com/locate/oregeorev

Predictive mapping for copper–gold magmatic-hydrothermal systems in NW Argentina: Use of a regional-scale GIS, application of an expert-guided data-driven approach, and comparison with results from a continental-scale GIS

R. Roy [a,b], D. Cassard [b,*], P.R. Cobbold [a], E.A. Rossello [c], M. Billa [b], L. Bailly [b], A.L.W. Lips [b]

[a] *Géosciences-Rennes (UPR 4661 du CNRS), Université de Rennes I, Campus de Beaulieu, 35042 Rennes Cedex, France*
[b] *BRGM, Mineral Resources Division, 3 avenue Claude Guillemin, BP 6009, 45060 Orléans Cedex 2, France*
[c] *CONICET and Departamento de Ciencias Geológicas, Universidad de Buenos Aires, 1428 Buenos Aires, Argentina*

Received 10 January 2005; accepted 11 October 2005
Available online 10 January 2006

Abstract

Geographic Information Systems (GISs) are very useful tools for managing, checking, and organizing spatial information–from many sources and of many types–in thematic layers. Processing of these data enables exploration-oriented GISs to produce potential and predictive maps for a given commodity, which constitute documents of real use in decision-making. Integration of all information in a single reference system enables a better understanding of the parameters controlling a region's metallogeny, in terms of both time and space. But what scale should be used for developing a mineral exploration GIS? Should preference be given to systems with high spatial resolutions (scale <1:500,000), or to more general systems with scales of around 1:1,500,000 or 1:2,000,000? Will the gain be worthwhile relative to the additional work generated by compilation at a higher scale? In order to make greater use of previous predictive studies performed on gold-rich epithermal and porphyry systems at the scale of the entire Andes, an expert-guided data-driven approach is now applied to a regional-scale GIS of NW Argentina, between the Puna and the Sierrras Pampeanas, where known deposits like Bajo de la Alumbrera, Agua Rica, and others, account for a metal potential of over 10 Mt Cu and 750 t Au. In developing this new predictive map, three criteria that were likely to be connected to the mineralizing event were selected and quantified: (i) lithostratigraphy, because of its role as a favourable environment for the development of mineralization, based on its physico-chemical properties; (ii) lithostratigraphic contacts, based on the rheological properties of the formations in contact; and (iii) the orientation of structural discontinuities, which channel source magmas and encourage the circulation of hydrothermal fluids. Assigning a score enables classification of the favourabilities calculated for each of the criteria considered. This approach is employed here to check and standardize the statistical results obtained by methods such as Weight of Evidence Modelling or an algebraic approach. For each criterion, four classes were distinguished: very favourable: score=3; favourable: score=2; slightly favourable: score=1; and unfavourable: score=0. The predictive map is obtained by adding the scores for the three favourable criteria defined above.

The regional-scale work identified 20 anomalous envelopes with cumulative scores greater than 5. They correspond to mining areas that are active (e.g., Bajo de la Alumbrera), under development (e.g., Agua Rica), or abandoned (e.g., La Mejicana), or to new

* Corresponding author. Tel.: +33 2 38 64 36 98; fax: +33 2 38 64 47 29.
E-mail address: d.cassard@brgm.fr (D. Cassard).

doi:10.1016/j.oregeorev.2005.10.002

areas (e.g., the Vicuña Pampa Volcanic Complex). Structural analysis of the region, integrating the orientation of the favourable envelopes, suggests that the mineralizing fluids were emplaced under extensional conditions, sub-parallel to the principal directions of shortening: (i) WNW–ESE, found along the southern edge of the Puna; and (ii) E–W, seen in the Sierra de Famatina. It appears that a regional-scale information system is a tool that is well suited to the definition of areas for mineral prospecting, and to the study and confirmation of metallotects usable for mineral exploration.

Comparison with work conducted on the basis of a 1:2,000,000 geological compilation shows that the principal mining districts can indeed be found at continental scale. On the other hand, the lack of detail inherent at a scale of 1:2,000,000 may lead to inaccuracies, in particular fictitious favourabilities assigned to formations that are genetically unrelated to the mineralization, but that contain, for example, small Tertiary intrusive bodies that cannot be recorded at this scale. This comparison therefore shows that the use of a continental-scale GIS is effective, and well suited to the definition of prospective areas at a strategic level.

Keywords: GIS; Multi-criteria processing; Metallogeny; Gold; Andean tectonics

1. Introduction

Geographic Information Systems (GIS) are very useful tools for managing spatial information. Coming as it does from sources of many kinds, such information is often heterogeneous in nature, quality, distribution, and density. However, once it has been checked and organized into thematic layers, an exploration-oriented GIS can produce predictive maps for a given commodity, and can be of great value in decision-making (e.g., Bonham-Carter et al., 1989; Bonham-Carter, 1994; Burrough and McDonnell, 1998; Billa et al., 2004). A GIS can also be a tool for research: once all the information is under a single reference system, the user can better explore the interactions between the various parameters that control the mineralization, and better define the laws governing the distribution of mineral concentrations in space and time (e.g., Cassard et al., 2003, 2004).

What is the best scale for developing a GIS for mineral exploration? Should one aim for good spatial resolution, at a detailed scale (>1:500,000) over a limited area (say, thousands of km^2); or should one take a more general view, at 1:1,500,000 or 1:2,000,000, covering a much larger area but including well-studied sites and zones of poorer information? Recent studies of multi-representational geographic bases, at multiple resolutions, have shown that the problems of changing scale are not trivial and are still far from being solved (Parent et al., 2000; Spaccapietra et al., 2000). To build a GIS, the user can choose between (1) the semi-continental approach, based on geodynamic criteria, an accuracy of the order of ± 2 km for geological contacts, deposits and prospects, and the plotting of calculations on pixels 10 km by 10 km square; or (2) the regional approach, which involves an accuracy much better than 1 km, detailed geology, detailed structural analyses, geophysical or geochemical surveys of limited areas (if available), and plotting on pixels 0.5 km by 0.5 km square.

In this paper, we describe a regional approach to studying the Famatina and Farallón Negro gold districts of NW Argentina with a two-fold objective:

1. In terms of methodology, we wished to investigate the predictive capacity of a regional GIS, as compared with that of a continental GIS. Using a similar methodology at continental scale, Billa et al. (2004) successfully identified the main Andean gold districts between Ecuador and Chile. At regional scale, would the resulting gain be worth the additional work of compilation? Although we might expect greater accuracy, when working on a smaller area, there will be fewer deposits for which information is reliable;
2. In terms of metallogeny, we wished to investigate the magmatic and structural controls on mineralization in a supra-subduction environment (Nelson, 1996). The continental approach had already yielded a strong positive correlation between (1) Neogene epithermal and porphyry gold deposits in the Central Andes and (2) gently dipping segments of the Benioff zone (Cassard et al., 2001; Billa et al., 2002). Would the regional approach yield a correlation with volcanic centres and with the major structural lineaments that are present in NW Argentina (Rossello et al., 1996b,c; Rossello, 2000)?

2. Geodynamic, geological, and metallogenetic setting of NW Argentina

2.1. Geodynamic setting of the Central Andes

From W to E, the main structural units of the Central Andes are the Cordillera Principal, the Pre-Cordillera,

the Puna, the Sub-Andean ranges, and the Sierras Pampeanas (Fig. 1). From north to south, the mountain belt becomes narrower (Jordan et al., 1983) and lower, in steps (Allmendinger et al., 1997).

Currently, the Nazca plate subducts beneath the South American plate in a nearly E–W direction and at a rate of 7.8 cm/year. From the Oligocene to the Early Miocene, convergence was more nearly NE–SW and much faster (on the order of 15 cm/year; Pardo-Casas and Molnar, 1987; Somoza, 1998). Currently, the dip of the subducting slab is on the order of 30°, to the N of latitude 27°S, becoming progressively more gentle to the S (Cahill and Isacks, 1992). Also from north to south, the continental lithosphere becomes thinner (Whitman et al., 1996) and the amount of horizontal shortening decreases (Isacks, 1988). Although there is now a gap in volcanic activity (Fig. 1) between latitudes 27°S and 33°S (Kay et al., 1999), magmatic activity has been intense here during the last 10 Ma (Fig. 2). During the Neogene, the Nazca plate may have flattened, causing a widening of the magmatic arc towards the east (Kay et al., 1999; Kay and Mpodozis, 2002). Along a few transverse lineaments (Salfity, 1985; Boudesseul et al.,

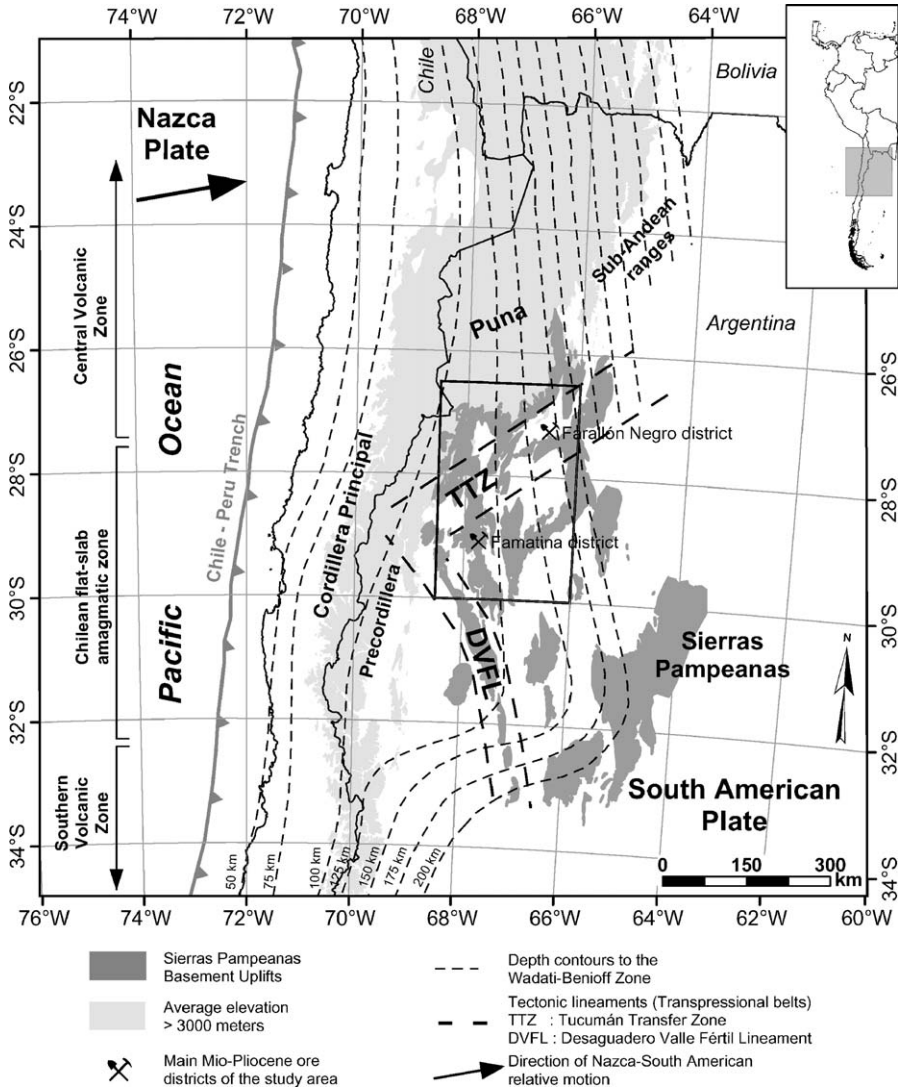

Fig. 1. Geodynamic setting illustrating main topographic features and subduction zone geometries of the Andes between 21°S and 34°S. Contours (in km) are for depth to Benioff zone (Cahill and Isacks, 1992), including Chilean flat slab (Jordan et al., 1983; Kay et al., 1999). Large arrow indicates direction of convergence between Nazca and South America (Pardo-Casas and Molnar, 1987; Somoza, 1998). In the study area (rectangle), main Miocene–Pliocene mining districts and major structural lineaments are indicated (Tucumán Transfer Zone—TTZ; de Urreiztieta, 1996; de Urreiztieta et al., 1996, and Desaguadero-Valle Fértil Lineament—DVFL; Rossello et al., 1996b).

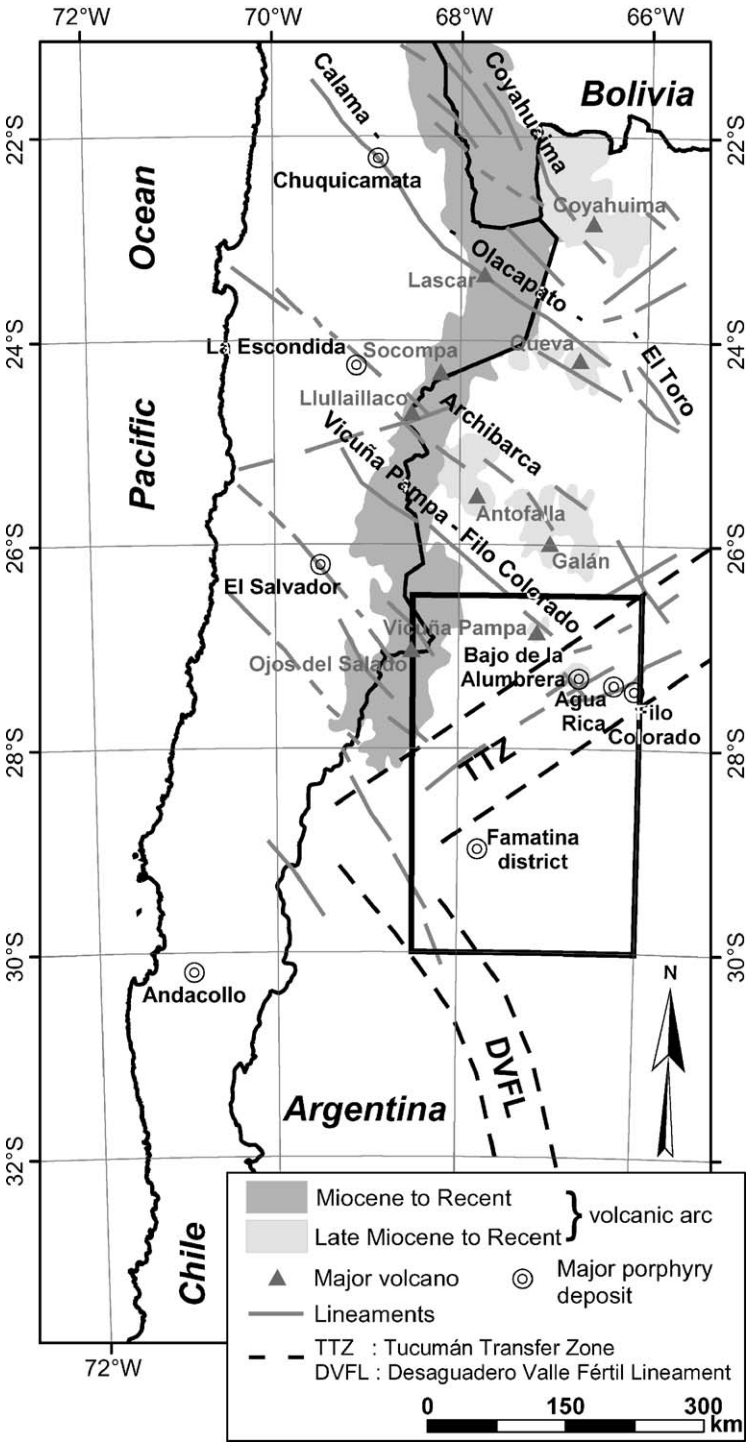

Fig. 2. Tectonic setting illustrating the distribution of Neogene volcanic rocks and main transverse lineaments. Major volcanic complexes and porphyry deposits lie along these lineaments (after Salfity, 1985; Boudesseul et al., 1999; Tosdal and Richards, 2001; Chernicoff et al., 2002; Matteini et al., 2002; Richards, 2003). The studied area is indicated by the rectangle.

1999), magmatic centres are developed more than 400 km from the trench. In Argentina, these include the Cerro Galán, Vicuña Pampa, and Farallón Negro volcanic complexes. The major porphyry deposits are also along these lineaments and close to the volcanic complexes (Fig. 2).

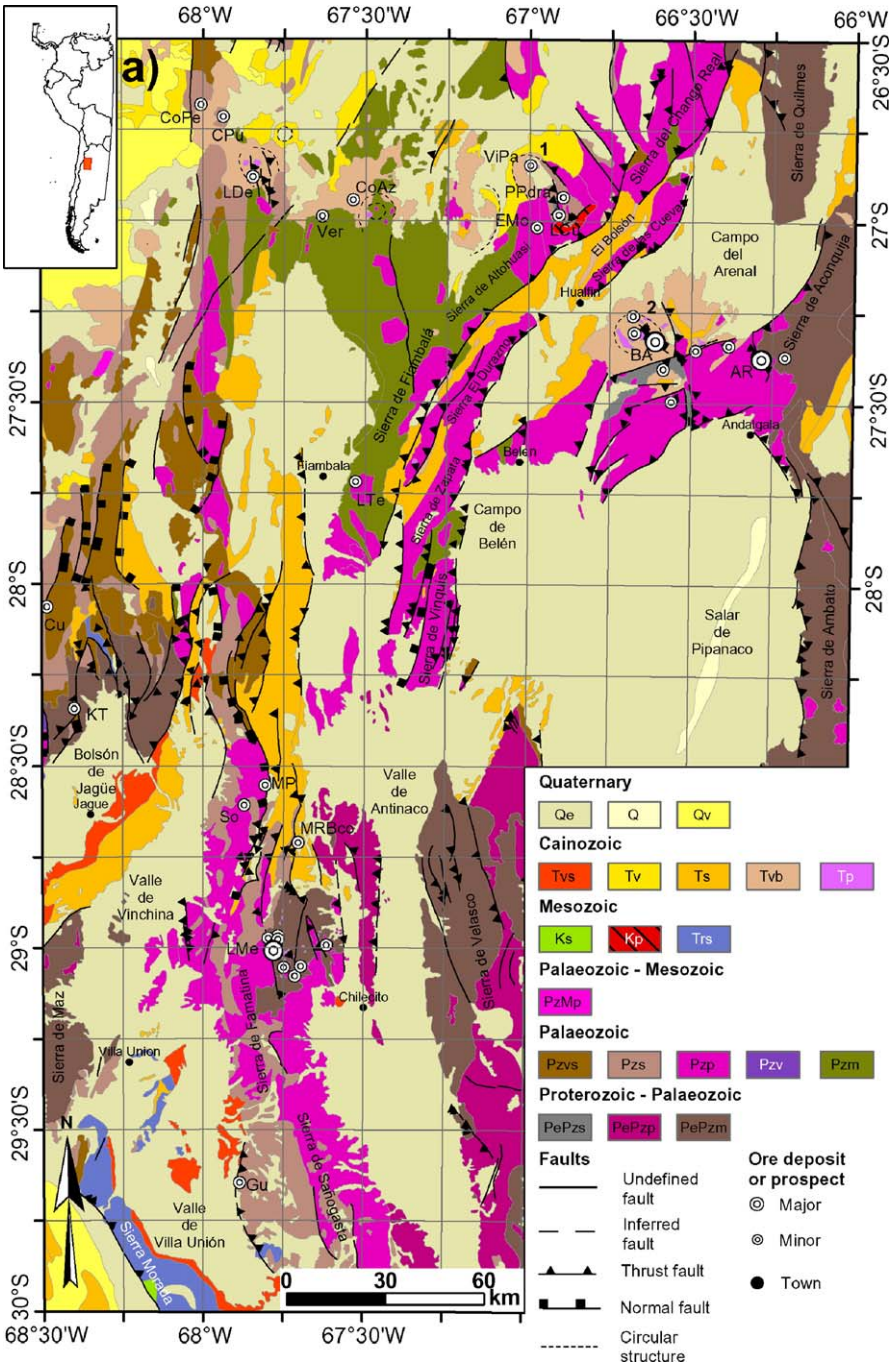

Fig. 3. Geological map of study area. Main map (a) shows lithology, structures, and ore deposits at regional scale. Enlargements focus on Farallón Negro Volcanic Complex (b) and Sierra de Famatina (c). For lithostratigraphic units, see Appendix A. Volcanic complexes are Vicuña Pampa (1) and Farallón Negro (2). Other localities are Alumbrera del Cerro Negro (ACoNo), Agua Rica (AR), Agua Tapada (AT), Bajo de la Alumbrera (BA), Bajo las Juntas (BJu), Bajo San Lucas (BSn), Capillitas (Ca), Cerro Atajo (CoAt), Cerro Azul (CoAz), Cerro Negro (CoNo), Cerro Peinado (CoPe), Cueros de Purulla (CPu), Cumichango (Cu), El Moradito (EMo), El Oro (EOr), El Pararrayo (EPa), El Tigre (ETi), Farallón Negro-Alto de la Blenda (FaNo-AB), Filo Colorado (FoCo), Gualcamayo (Gu), King Tud (KT), La Cuesta (LCu), La Descubridora (LDe), La Mejicana (LMe), Las Termas (LTe), Los Bayitos (LBa), Mal Paso (MP), Mogote Rio Blanco (MRBco), Montey (Mo), Offir (Off), Puerto Piedra (PPdra), Sotran (So), Vernacua (Ver) and Vicuña Pampa (ViPa). The map projection for all layers is Transverse Mercator, Datum WGS 84, centred on meridian 68°W.

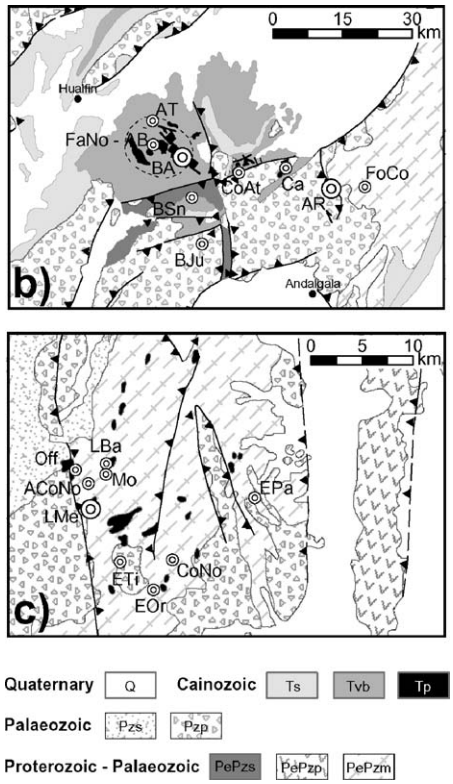

Fig. 3 (*continued*).

2.2. Geological and structural setting of NW Argentina

2.2.1. Geological setting

Crystalline basement crops out in the Sierras Pampeanas. It consists of metamorphic rocks (e.g., schists, gneisses, orthogneisses, and migmatites) and granites of Precambrian to late Palaeozoic age (Fig. 3a). According to Ramos (1999), these rocks result from tectonic accretion of microcontinents at the western margin of Gondwana, during the Famatinan orogeny (465 to 385 Ma) and the Gondwanan orogeny (290 to 250 Ma).

During the Mesozoic, back-arc extension prevailed in southwestern Gondwana (Ramos, 1999), its effects reaching as far west as what is now the Atlantic margin (Rossello and Mozetic, 1999). However, in NW Argentina outcrops of Mesozoic rocks are rare and of limited extent (Fig. 3a). Examples are Triassic sandstones and shales, on the southwestern side of the Sierra de Famatina, and Cretaceous basalts within continental sandstones, near Belén on the southern side of the Campo del Arenal (Rossello and Mozetic, 1999).

During the Neogene, Andean compression resulted in a series of alternating basement blocks and basins, as in the Rocky Mountains of the western USA (Jordan and Allmendinger, 1986). Erosion of the mountains produced detritus, which progressively filled the developing basins. On the western edge of the study area, in the Bolsón de Jagüe, the resulting detrital sequence is up to 15 km thick; and in the north, on the edge of the Puna plateau, the El Bolsón basin contains up to 5 km of interbedded sediment and volcanic rocks. Tertiary volcanic rocks crop out only in the northern part of the study area (Fig. 3a). Ignimbrites and andesitic and dacitic lava flows are all that remain of former stratovolcanoes at Vicuña Pampa (Rossello, 1980) and Farallón Negro (Fig. 3a and b). Into these rocks and into the Palaeozoic basement, dacitic to monzonitic magmas intruded, forming stocks. Magmatic activity reached a climax during the Late Miocene and Early Pliocene (Sasso and Clark, 1998). Its products are numerous along the Vicuña Pampa–Filo Colorado lineament, which trends NW–SE (Figs. 2 and 3b), parallel to other tectonic lineaments (Salfity, 1985; Boudesseul et al., 1999) and to magnetic lineaments (Chernicoff et al., 2002). To the south, although volcanic rocks are scarce or absent, there are hypovolcanic intrusions of Pliocene age (Losada-Calderón et al., 1994) in Early Cainozoic sedimentary sequences (for example, at Mogote Rio Blanco) and in Palaeozoic basement (for example, in the Sierra de Famatina, Fig. 3c).

2.2.2. Structural setting

In the Sierras Pampeanas and Puna, thick-skinned faults involve the crystalline basement (Jordan et al., 1983; Kley et al., 1999); whereas in the Sub-Andes, between latitudes 15°S and 27°S, thin-skinned thrusts have formed within the cover rocks of the main foreland basin (Allmendinger et al., 1997).

Marking a transition between the southern Puna and northern Sierras Pampeanas is the Tucumán lineament (Mon, 1976) or Tucumán Transfer Zone (TTZ, Fig. 1; de Urreiztieta, 1996; de Urreiztieta et al., 1996). This NE–SW zone, about 100 km wide, was formed under right-lateral transpression. To the SW, the NNW–SSE Desaguadero-Valle Fértil Lineament (DVFL; Rossello et al., 1996b,c) formed under left-lateral transpression. At the restraining intersection of these two transpressional structures is the Umango-Maz uplift, which trends N–S (Sierra de Maz, Fig. 3a; Rossello et al., 1996b). Parallel to it are other ranges, bounded by deep-seated reverse faults. These have opposing vergences in the Sierra de Famatina and an easterly vergence in the Sierra de Velasco. Summits become progressively lower towards the east, suggesting that the amount of thrusting diminishes in this direction (Fig. 1; Rossello et al., 1996b).

Although the region as a whole is seismically active, earthquakes are most numerous at the edge of the Puna. From their focal mechanisms, the greatest stress is horizontal and perpendicular to the edge of the plateau (Assumpção and Araujo, 1993; Fig. 4a). Along the southern edge of the Puna, Neogene and currently active faults form two families (de Urreiztieta, 1996; de Urreiztieta et al., 1996; Fig. 4b). To account for the first family, the greatest stress trends N080°E, sub-parallel to the direction of convergence between the Nazca and South American plates. To account for the second family, the greatest stress trends N140°E, sub-perpendicular to the southern edge of the Puna. Probably, the first family results mainly from an intra-plate stress field, whereas the second family results mainly from gravity spreading of the plateau (Assumpção and Araujo, 1993) and right-lateral transpression along the Tucumán Transfer Zone (de Urreiztieta, 1996; Rossello et al., 1996a; Marques and Cobbold, 2002). In general, the principal directions of stress and of shortening must have varied in space and time, depending on the relative magnitudes of these components.

Many of the Neogene faults formed by reactivation of older structures. Notable examples are Mesozoic normal faults, trending NE–SW to NW–SE (Rossello

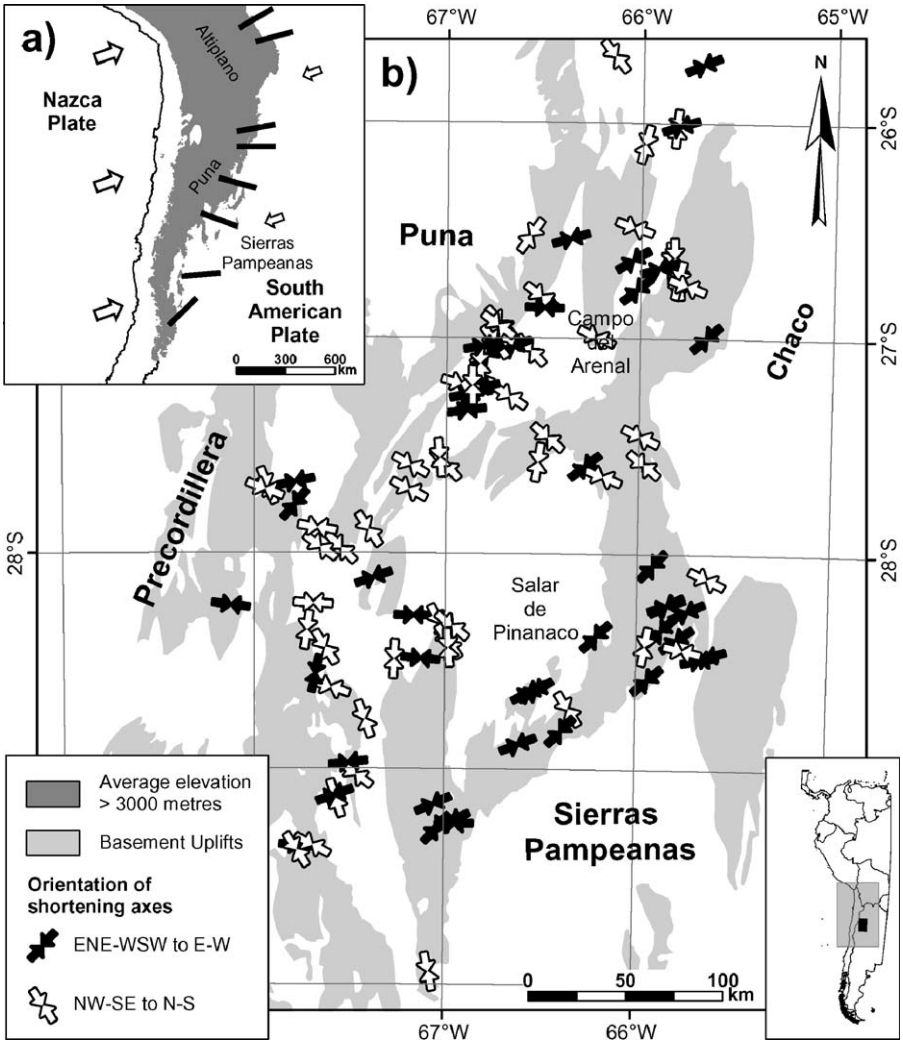

Fig. 4. (a) Mean direction of greatest horizontal stress (black bold lines), calculated from earthquake focal mechanisms at edge of Altiplano (Assumpção and Araujo, 1993). Also shown are directions of convergence between Nazca and South America (large white arrows) and of absolute motion of South America (small white arrows). (b) Kinematic analysis of fault-slip data across Sierra Pampeanas and southern edge of Puna (from de Urreiztieta, 1996; de Urreiztieta et al., 1996). Shortening axes trend NW–SE to N–S (white arrows) at edge of Puna and in Tucumán Transfer Zone (TTZ). More regionally, they trend ENE–WSW to E–W (black arrows), sub-parallel to direction of plate convergence.

and Mozetic, 1999), and Palaeozoic reverse faults, trending N–S to NW–SE (Ramos, 1999).

2.3. Metallogenetic setting

In the area studied (Fig. 3), 34 occurrences (deposits or showings) contain gold, either as the main mineral or as a by-product (Table 1). Of these occurrences, 22 are of Cainozoic age, 3 of Mesozoic age, 3 of Palaeozoic age, and 6 of unconstrained age. Moreover, 64% of the ore deposits that contain gold are of porphyry type (10 occurrences) or related to shallow intrusions (12 occurrences). The main gold-bearing occurrences in the foreland of the Cordillera Principal formed during the Late Cainozoic, as the volcano-magmatic arc widened towards the east (Sasso and Clark, 1998).

Near latitude 27°S on the TTZ, Farallón Negro is Argentina's biggest gold district (Figs. 1 and 3a and b). Production is under way at Bajo de la Alumbrera [767 Mt of reserves at 0.51% Cu and 0.64 g/t Au (Angera, 1999)] and Farallón Negro [1.5 Mt with grades of ~6 g/t Au and 99 g/t Ag (BRGM, 2001)]. Other occurrences are under evaluation, e.g., Agua Rica [1,457 Mt of measured and indicated reserves at 0.2% Cu cutoff grading 0.44% Cu, 0.03% Mo, 0.19 g/t Au, and 3 g/t Ag (electronic communication, Northern Orion website)]. Neogene mineralization in this district is associated with porphyry intrusions (e.g., Bajo de la Alumbrera) or andesites.

In the Sierra de Famatina (Fig. 1; Fig. 2b), between the TTZ and the DVFL, are the mining districts of La Mejicana [300 Mt at 0.06% Mo, 0.37% Cu, and 0.9 g/t Ag (Mayón, 1999)] and El Oro [200,000 t at 5.8 g/t Au and 0.37% Cu (Brodtkorb and Schalamuk, 1999)]. Gold mineralization concentrates around porphyry intrusions of dacitic to andesitic composition in a basement of metamorphic rocks and Palaeozoic granitoids (e.g., La Mejicana). In contrast to Farallón Negro, Tertiary volcanic rocks are rare or absent. An alteration zone, more than 20 km wide, is visible on satellite images of La Mejicana (NASA, S-19-25, 2000).

From geochronological data ($^{40}Ar/^{39}Ar$, K/Ar, or Apatite Fission Track), we infer that gold mineralization occurred after a magmatic phase and in the early stages of a compressional tectonic phase (Table 2). Kay et al. (1999) deduced a similar timing for Cu–Au porphyry-type deposits in Chile.

In the northern part of the area studied, at the Bajo de la Alumbrera, Farallón Negro, and Agua Rica deposits, the mineralization is of Middle Miocene to Early Pliocene age (Sasso and Clark, 1998), whereas to the south, at La Mejicana, it is of Pliocene age (Losada-Calderón et al., 1994).

3. Construction of a regional-scale gold deposit model: methodology

3.1. Available data and format

In our study at 1:500,000, we constructed a deposit model from vector data of point type ("deposits" layer), line type ("tectonic structures" layer and "lithostratigraphic contacts" layer), and polygon type ("lithostratigraphy" layer).

The "deposits" layer was extracted from GIS Andes (Cassard, 1999a,b; BRGM, 2001), at a scale of 1:2,000,000. Because of the change in scale, it was necessary to improve the georeferencing of the deposits, and to update the database, adding prospects not shown at 1:2,000,000. The attributes used were location, age of mineralization, deposit type, and ore paragenesis. Information on metal content was not used, because it was considered too fragmentary. A total of 34 prospects and deposits hosting gold (as a main mineral or by-product) were used to calculate favourability.

Information for the "lithostratigraphy" layer came from maps at 1:500,000 for the provinces of Tucumán (González et al., 1994), Catamarca (Martínez et al., 1995), and La Rioja (Guerrero et al., 1993), and at 1:200,000 for the areas of Bajo de la Alumbrera (González Bonorino, 1947) and Famatina (Turner, 1971). For easy comparison with previous work, the groupings and geological codes[1] assigned to the polygons (see Appendix A) are those used by Billa et al. (2004) for GIS Andes, and not the ones from the original geological maps.

From the "lithostratigraphy" layer, we generated a "lithostratigraphic contacts" layer. Each family of contacts is identified by a code for the two lithologies in contact. This layer is intended to show the importance of lithological interfaces, which may produce barrier effects or alternatively drain effects, encouraging the trapping of mineralization.

For the "tectonic structures" layer, we extracted faults from 1:500,000 maps of Catamarca (Martínez et al., 1995) and La Rioja (Guerrero et al., 1993), and from 1:200,000 maps of NW Argentina (González Bonorino, 1947; Turner, 1971). Additional data came from our field studies and from Landsat images

[1] All the codes are available for consultation at the following address: http://gisandes.brgm.fr/gis_geol_legend.htm.

Table 1
Mineral deposits containing gold as main commodity or by-product and used for favourability calculations

District	Deposit	Lithostratigraphic unit	Stratigraphic age	Deposit type	Gold production	Tonnages (Mt)	Cu (%)	Au (g/t)	References
Catamarca Province									
Agua de Dionisos	Agua Tapada	Tp	Cainozoic	Syn-, late-orogenic veins	Main commodity			0.5	Alderete, 1999a
Agua de Dionisos	Bajo de la Alumbrera	Tp	Late Miocene	Porphyry	Main commodity	767	0.51	0.64	Sasso and Clark, 1998; Angera, 1999; Godeas et al., 1999; Proffett, 2003
Agua de Dionisos	Bajo de San Lucas	Tp	Cainozoic	Porphyry	By-product		0.26	0.35	Sasso and Clark, 1998; Alderete, 1999b
Agua de Dionisos	Bajo Las Juntas	Tp	Cainozoic	Porphyry	Main commodity				Sasso and Clark, 1998
Agua de Dionisos	Farallón Negro-Alto de la Blenda	Tp	Late Miocene	Epithermal LS	Main commodity	0.48		6.1	Sasso and Clark, 1998; Alderete, 1999c
	Alumbrera del Cerro Negro	PePzm	Early Pliocene	Porphyry	Main commodity				BRGM, 2001
	Agua Rica (Mi Vida)	Tp	Late Miocene	Porphyry	Main commodity	1457	0.44	0.19	Electronic communication, Northern Orion website, 2005
	Cerro Negro	PePzm	Early Pliocene	Epithermal LS	Main commodity				BRGM, 2001
	Filo Colorado	Tp	Early Miocene	Porphyry	Main commodity	9	0.3–0.5	0.02	Guillou, 1999; Godeas et al., 1999
Capillitas	Capillitas	Tp	Early Pliocene	Epithermal LS	By-product	0.39	2.32	2.66	Sasso and Clark, 1998; Marquez-Zavalia, 1999; Godeas et al., 1999
Cerro Atajo	Cerro Atajo	Tp	Early Miocene	Porphyry	Main commodity	<0.04	0.41–5	2–2.7	Sasso and Clark, 1998; Peralta, 1999; Godeas et al., 1999
	Cerro Azul	Tvb	Pliocene	Veins in shallow-depth intrusion	By-product	0.003		3.7	Godeas et al., 1999; BRGM, 2001
	Cerro Peinado	Tvb	Unspecified	Veins in shallow-depth intrusion	Main commodity				BRGM, 2001
	Cueros de Purulla	Pzs	Miocene–Pliocene	Veins in shallow-depth intrusion	Main commodity				BRGM, 2001
	Cumichango	Pzvs	Unspecified	Unspecified	By-product				BRGM, 2001

Culampaja	El Moradito	Pzp	Carboniferous	Shear-zones	Main commodity			10.2	Avila et al., 1999a
	El Oro	PePzm	Early Miocene	Syn-, late-orogenic veins	Main commodity	0.2	0.37	5.8	Passarello et al., 1992; Brodtkorb and Schalamuk, 1999; Mayón, 1999; Godeas et al., 1999
	El Pararrayo	PePzm	Cainozoic	Veins in basic intrusions	Main commodity				Mayón, 1999
	El Tigre	Pzp	Early Pliocene	Epithermal LS	Main commodity				Mayón, 1999
	Gualcamayo	Pzs	Unspecified	Skarn	Main commodity	0.65		6.0	Gemuts et al., 1996; Godeas et al., 1999
	La Cuesta	Pzs	Mesozoic (?)	Unspecified	Main commodity				BRGM, 2001
La Hoyada	La Descubridora	Tvb	Mio–Pliocene	Veins in shallow-depth intrusion	Main commodity	0.67	0.1–3.9		Ricci et al., 1999
La Rioja Province									
Valle Hermoso	King Tut	PePzm	Silurian/Cainozoic (?)	Syn-, late orogenic veins	Main commodity	0.005		5.9	Lapidus and Padula, 1982
Mogote Rio Blanco	Mogote Rio Blanco	Tp	Cainozoic	Veins in shallow-depth intrusion	Main commodity		1.5	5–6	BRGM, 2001
	La Mejicana	TP	Early Pliocene	Epithermal HS	Main commodity				Mayón, 1999
	Los Bayitos	PePzm	Cainozoic	Porphyry	By-product				Brodtkorb and Schalamuk, 1999; Mayón, 1999
	Montey	PePzm	Cainozoic	Porphyry	Main commodity				Brodtkorb and Schalamuk, 1999; Mayón, 1999
Offir	Offir	PePzm	Cainozoic	Porphyry	Main commodity	0.06		14.9	Brodtkorb and Schalamuk, 1999; Mayón, 1999; Godeas et al., 1999
	Las Termas	Pzp	Palaeozoic	Peri-granitic veins and greisens	By-product				Avila et al., 1999b
	Mal Paso	Pzp	Unspecified	Syn-, late orogenic veins	Main commodity				Mayón, 1999
	Puerto Piedra	Pzs	Mesozoic (?)	Unspecified	Main commodity				Garcia and Rossello, 1984
	Sotran	Pzp	Unspecified	Syn-, late orogenic veins	Main commodity				BRGM, 2001
	Vernancua	Pzm	Unspecified	Veins in shallow-depth intrusion	Main commodity				BRGM, 2001
	Vicuña Pampa	Tp	Cainozoic	Unspecified	Unspecified				Rossello, 2000

For lithostratigraphic units, see Appendix A. Deposits may be of Low Sulphidation (LS) or High Sulphidation (HS).

Table 2
Chronology of magmatic, tectonic, and mineralizing events in NW Argentina

Period	Dating method	Geological event	Locality	Reference
Sierra de Famatina				
From 4.50 to 4.19 Ma	AFT	Uplift and cooling by exhumation	Sierra de Famatina	Coughlin et al., 1998
From 4.84 ± 0.41 to 4.19 ± 0.27 Ma	$^{40}Ar/^{39}Ar$	Alteration and high sulphidation vein system	Famatina District	Losada-Calderón et al., 1994
From 6.38 ± 0.37 to 4.24 ± 0.11 Ma	K/Ar	Magmatic activity	Sierra de Famatina (El Durazno-La Estrechura)	Toselli, 1996
Sierra de Aconquija and Sierra del Chango Real				
2.7 ± 0.8 Ma	K/Ar	Supergene enrichment	Farallón Negro-Alto de la Blenda deposit	McBride, 1972; Sasso and Clark, 1998
5.35 ± 0.14 Ma	$^{40}Ar/^{39}Ar$	High-sulphidation epithermal assemblage	Agua Rica deposit	Sasso and Clark, 1998
6.10 ± 0.04 Ma	$^{40}Ar/^{39}Ar$	Stockwork-controlled phyllic alteration	Farallón Negro District	Sasso and Clark, 1998
From 7.6 to 6.0 Ma	AFT	Uplift and cooling by exhumation	Sierra de Aconquija	Coughlin et al., 1998
8.56 ± 0.48 Ma	$^{40}Ar/^{39}Ar$	Magmatic activity	Agua Rica (Melcho stock)	Sasso and Clark, 1998
From 8.75 ± 0.07 to 8.41 ± 0.08 Ma	$^{40}Ar/^{39}Ar$	Volcanic eruption	Cerro Atajo	Sasso and Clark, 1998
From 12.56 ± 0.36 to 8.59 ± 0.10 Ma	$^{40}Ar/^{39}Ar$	Volcanic and magmatic activity	Farallón Negro Volcanic Complex	Sasso and Clark, 1998
From 25.0 ± 1.0 to 14.0 ± 0.5 Ma	K/Ar	Volcanic and magmatic activity	Vicuña Pampa Volcanic Complex	Rossello, in press
From 38.0 ± 3.0 to 29.0 ± 3.0 Ma	AFT	Uplift and cooling by exhumation	Sierra del Chango Real	Coutand et al., 2001

AFT: Apatite Fission-Track (AFT).

(NASA, S-19-25, 2000). The attribute that we adopted for calculating favourability is fault trend (in class intervals of 10°). Fault-slip data do not make good attributes, because the information is fragmentary and unevenly distributed.

3.2. Data preparation

The processing phase requires transforming the polygons on the "lithostratigraphy" vector layer into a grid of pixels, to be used as a counting surface. Since all the data are at a scale of 1:500,000 (the scale of the geological compilation and the plotting of deposit and prospect locations), the pixel size is 500 × 500 m (1 mm^2 on the 1:500,000 map). The small pixel size limits the placement errors, which may otherwise occur during the transfer of calculated information with reference to fixed points when the counting pixels are large in size.

The data were processed with ArcView Spatial Analyst ESRI® software and two plug-in extensions for multi-criteria approaches, SynArc BRGM® (Braux, 1996) and Arc-SDM (Kemp et al., 2001). The information was captured at a scale of 1:500,000. The projection for all layers was Transverse Mercator, Datum WGS-84, centred on 68°W.

3.3. Processing

The processing procedure was in three stages: (i) identification of criteria that are relevant and can be used in the calculations, (ii) quantification of the selected criteria, and (iii) compilation and production of the metallogenic map, predictive for deposit spatial distribution.

3.3.1. Stage 1: identification of criteria

The three main parameters, which carry sufficient information at this scale, provide uniform coverage, and may correspond to metallotects that control the distribution of mineralization (Table 1), are (1) lithostratigraphy of the country rock, (2) faults, and (3) lithostratigraphic contacts. Major regional structures were not considered in the calculation phase, because they are too poorly defined in extent (especially in width).

3.3.1.1. Lithostratigraphy of the country rock. Some mineralization is genetically related to one type of host rock. This is particularly true for porphyry deposits (e.g., Bajo de la Alumbrera, Agua Rica) and their associated epithermal manifestations. However, one of the problems encountered is the size of these mineral-bearing intrusions: their outcrop size or related alter-

ation halo may be extremely small (e.g., less than 1 km^2 at Bajo de la Alumbrera; J. Angera, personal communication), making their plotting progressively more difficult as the scale of the geological compilation decreases. Thus for intrusions that are small or that do not crop out, the favourability might be assigned to a country rock polygon whose lithostratigraphy has no direct connection with the mineralization. Such a lithostratigraphy–with no genetic link to the mineralization–may nevertheless, as a country rock, be favourable to the development of mineralization, because of its physico-chemical properties (rheology, porosity, composition, etc.) (Table 3).

3.3.1.2. Faults. In metallogeny, the presence of structural discontinuities is generally considered to be a major criterion for the presence of deposits. Faults facilitate the passage of source magmas and the circulation of hydrothermal fluids (e.g., Wyborn et al., 1994; Sillitoe, 1997; Oyarzún, 2000; Hanuš et al., 2000) (Table 4).

3.3.1.3. Contacts between lithostratigraphies of different types. The proximity of some lithostratigraphic contacts is empirically considered to be favourable for the presence of mineralization. Rheological contrasts may favour fracturing and the formation of openings, followed by the channeling and trapping of mineralized fluids (Castaing et al., 1993; Sillitoe, 1997) (Table 5).

3.3.1.4. Regional geological structures (magmatic, volcanic, or structural axes). Mineralization is frequently associated with major tectonic or magmatic corridors. The superposition (or intersection) of several metallotects generally enhances favourability (Routhier, 1980). Such structures are shown on the predictive map, but were not used in the calculation phase for the reasons mentioned above.

The next stage consists of assessing–essentially by statistical and probabilistic methods–the representation of these criteria in the vicinity of the deposits studied, and thereby their potential contribution to the genesis of mineral concentrations.

3.3.2. Stage 2: quantification of criteria

This stage consists of assigning a numerical value to each of the criteria previously selected, aiming to avoid over- or under-valuing certain relationships, and then mapping them over the entire area studied. Several

Table 3
Results for "country rock lithostratigraphy" criterion, using weight of evidence method (WofE; Bonham-Carter, 1994), and favourability scores for various geological formations

Lithostratigraphic units	Area (km^2)	Area (%)	Number of deposits in this unit	% of Deposits	W^+	W^-	Contrast ($W^+ - W^-$)	Score
Q	48,367.506	50.61	0	0	–	–	–	0
Qe	455.169	0.48	0	0	–	–	–	0
Qv	2372.709	2.48	0	0	–	–	–	0
QTv	586.413	0.61	0	0	–	–	–	0
Ts	4968.035	5.20	0	0	–	–	–	0
Tvs	719.012	0.75	0	0	–	–	–	0
Tv	1187.610	1.24	0	0	–	–	–	0
Tvb	2387.670	2.50	3	9	1.26	−0.07	1.33	2
Tp	92.214	0.10	12	35	6.04	−0.43	6.48	3
Ks	18.768	0.02	0	0	–	–	–	0
Kp	39.894	0.04	0	0	–	–	–	0
Trs	733.718	0.77	0	0	–	–	–	0
PzMp	26.104	0.03	0	0	–	–	–	0
Pzs	4092.923	4.28	4	12	1.01	−0.08	1.09	2
Pzv	10.438	0.01	0	0	–	–	–	0
Pzvs	2703.257	2.83	1	3	0.04	0.00	0.04	1
Pzp	9335.375	9.77	5	15	0.41	−0.06	0.47	1
Pzm	3940.241	4.12	1	3	−0.34	0.01	−0.35	0
PePzs	133.118	0.14	0	0	–	–	–	0
PePzp	4046.621	4.23	0	0	–	–	–	0
PePzm	8841.189	9.25	8	24	0.93	−0.17	1.11	2
Sebkha	515.011	0.54	0	0	–	–	–	0
Total	95,572.994	100.00	34	100				

Scores are 0 (unfavourable), 1 (slightly favourable), 2 (favourable), and 3 (very favourable). For method of calculation, see Table 6.

Table 4
Results for "fault trend" criterion, using algebraic method (Knox-Robinson and Groves, 1997), and favourability scores for various trend classes

Class	Cumulative length, Length_i (km)	$\text{Lr}_i = \frac{\text{Length}_i}{\text{Length}_{\text{tot}}}(\%)$	n_i	$\text{Pr}_i = \frac{n_i}{N_{\text{tot}}}(\%)$	Fav_i	Score
0–10°	948.480	13.03	1.99	3.28	−1.38	0
10–20°	1037.020	14.25	2.35	3.87	−1.30	0
20–30°	715.783	9.84	0.44	0.73	−2.61	0
30–40°	507.839	6.98	1.00	1.65	−1.44	0
40–50°	407.974	5.61	4.94	8.15	0.37	1
50–60°	157.699	2.17	1.90	3.13	0.37	1
60–70°	100.165	1.38	4.07	6.71	1.58	3
70–80°	119.705	1.65	2.65	4.37	0.98	2
80–90°	32.777	0.45	1.00	1.65	1.30	3
90–100°	34.804	0.48	0.71	1.17	0.90	2
100–110°	66.452	0.91	3.07	5.06	1.71	3
110–120°	43.947	0.60	0.00	0.00	0.00	0
120–130°	50.205	0.69	2.27	3.74	1.69	3
130–140°	279.790	3.85	4.16	6.86	0.58	1
140–150°	359.430	4.94	8.00	13.19	0.98	2
150–160°	561.203	7.71	5.67	9.35	0.19	1
160–170°	832.540	11.44	7.43	12.25	0.07	1
170–180°	1020.884	14.03	9.00	14.84	0.06	1
Total	7276.697	100.00	60.65	100.00		

Scores are 0 (unfavourable), 1 (slightly favourable), 2 (favourable), and 3 (very favourable). For method of calculation, see Table 6.

methods are available for doing this (see reviews in Knox-Robinson and Groves, 1997; Lips et al., 2002; Billa et al., 2004).

• The Boolean method. For a given criterion, each of the elements on the map is either favourable or unfavourable for the presence of a deposit.

• The "knowledge-driven" approach. This is based on the knowledge and experience of the geologist, and seeks to find an association of favourable criteria in a study area. It employs methods such as fuzzy logic or the Dempster-Shafer belief functions, and is based on models of existing or conceptual deposits.

• The "data-driven" approach. This is based on the quantification of relationships between the criteria and the known deposits. Statistical methods use techniques such as regression, weights of evidence (WofE; Bonham-Carter, 1994), neural networks (cf. Brown et al., 2000; Bougrain et al., 2003) and data mining (cf. Salleb and Vrain, 2000; Salleb, 2003). The algebraic methods (Knox-Robinson and Groves, 1997) attempt to determine a deposit or occurrence density or a contained metal density per unit of area (or of length), thereby getting around certain limitations of WofE when applied to geological maps, so as to avoid the requirement of conditional independence and allow deposit size to be incorporated into the assessment.

• The hybrid "expert-guided data-driven" approach. This combines two of the above approaches, so as to take advantage of their respective benefits. During the preliminary phases of WofE, performed on lithostratigraphy, it was found that the presence of Tertiary intrusions is a very strong determining criterion. It masks all the other criteria likely to signal mineralization. However, it is highly probable that certain favourable Tertiary intrusions or hydrothermal alteration zones are not incorporated at a scale of 1:500,000, or have not been identified. So in order to take into account more subtle distribution criteria that are nevertheless likely to point towards new mineralized areas, an assessment and scoring operation was performed, based on calculated favourabilities (WofE and densities) for the various evidential themes (in the specialized language of GIS, an evidential theme is a map or area layer, in either vector or raster format, used for prediction of point objects, such as mineral occurrences): very favourable = 3; favourable = 2; slightly favourable = 1; and unfavourable = 0. These favourability scores were then added on a compilation ("predictive") map, where the values range from 0 (unfavourable) to a maximum value equal to the sum of the favourable scores.

3.3.2.1. Quantification of lithostratigraphy criterion. The method selected for quantifying the lithostratigraphy criterion is the WofE, which is a probability-based approach (Bonham-Carter, 1994) that uses Bayes' rule

Table 5
Results for "lithostratigraphic contacts" criterion, using algebraic method (Knox-Robinson and Groves, 1997), and favourability scores for various classes of contacts

Lithostratigraphic contacts	Cumulative length, Length_i (km)	$\text{Lr}_i = \frac{\text{Length}_i}{\text{Length}_{\text{tot}}}(\%)$	n_i	$\text{Pr}_i = \frac{n_i}{N_{tot}}(\%)$	Fav_i	Score
Tp–Tp	1.028	0.01	1.33	1.65	5.29	3
Pzs–Tp	1.961	0.02	0.89	1.10	4.24	3
Pzp–Tp	36.489	0.30	9.01	11.15	3.63	2
PePzs–Tp	4.265	0.03	1.00	1.24	3.58	2
PePzm–Tp	70.321	0.57	12.54	15.52	3.30	2
PePzs–Pzs	9.133	0.07	1.54	1.90	3.25	2
Tp–Ts	7.780	0.06	1.00	1.24	2.98	2
Q–Tp	11.091	0.09	0.94	1.16	2.56	0[a]
Tp–Tvb	111.546	0.90	8.81	10.90	2.49	2
PePzs–Tvb	32.087	0.26	2.04	2.53	2.27	2
Kp–Pzs	15.723	0.13	1.00	1.24	2.27	2
Kp–Pzp	3.967	0.03	0.16	0.20	1.85	1
PePzm–Pzp	407.979	3.30	11.29	13.97	1.44	1
Pzp–Tvb	180.177	1.46	4.06	5.03	1.24	1
PePzs–Pzp	63.894	0.52	1.31	1.62	1.14	1
Pzs	36.644	0.30	0.69	0.85	1.05	1
Pzs–Tvb	103.310	0.84	1.88	2.33	1.02	1
Pzs–Ts	115.714	0.94	1.77	2.19	0.85	1
Ts–Ts	74.989	0.61	1.00	1.24	0.71	1
PePzm–Pzs	115.026	0.93	1.19	1.48	0.46	1
Pzp–Pzp	93.138	0.75	0.96	1.18	0.45	1
PePzm–Pzvs	101.286	0.82	0.79	0.98	0.18	1
Pzm–Tvb	162.296	1.31	1.00	1.24	−0.06	0
Pzp–Pzs	850.882	6.89	4.74	5.86	−0.16	0
Q–Tvb	503.180	4.08	1.23	1.52	−0.99	0
Pzm–Pzp	434.433	3.52	1.00	1.24	−1.05	0
Pzs–Pzvs	483.850	3.92	1.00	1.24	−1.15	0
Pzs–Q	1393.472	11.29	1.85	2.28	−1.60	0
Pzp–Ts	397.496	3.22	0.44	0.55	−1.77	0
Pzs–Pzs	118.862	0.96	0.13	0.16	−1.81	0
PePzm–Q	1430.717	11.59	1.39	1.72	−1.91	0
Pzp–Q	2013.994	16.31	1.74	2.15	−2.03	0
Ts–Tvb	196.545	1.59	0.13	0.16	−2.29	0
Q–Ts	2095.159	16.97	0.78	0.97	−2.86	0
Pzm–Q	666.926	5.40	0.19	0.24	−3.12	0
Total	12,345.357	100.00	80.81	100.00		

Scores are 0 (unfavourable), 1 (slightly favourable), 2 (favourable), and 3 (very favourable). For method of calculation, see Table 6.
[a] See explanation in the text.

to combine evidence with an assumption of conditional independence. Where sufficient data are available, it can be applied to estimate the relative importance of evidence by statistical means.

Calculating it on a geological map, covering several geological formations, is similar to using a multi-class evidential theme. At the end of the calculation, three numerical values are selected to characterize each geological formation (see Bonham-Carter, 1994; Kemp et al., 2001 for details of these calculations). The positive and negative weights (written W^+ and W^-) provide a measure of the spatial association between the training points (in this case the mineral deposits) and the evidential theme (Eqs. (1) and (2)). A weight is calculated for each class of the evidential theme:

$$W^+(B) = \ln\left(\frac{P(B|D)}{P(B|\bar{D})}\right) \tag{1}$$

$$W^-(B) = \ln\left(\frac{P(\bar{B}\,|D)}{P(\bar{B}|\bar{D})}\right). \tag{2}$$

In this equation: D is the number of unit cells containing a prospect or deposit (training point); B is the number of unit cells containing a given formation b;

$P(B \mid D)$ is the probability of occurrence of formation b, given the condition of being on a deposit; $P(B \mid \bar{D})$ is the probability of occurrence of formation b, given the condition of not being on a deposit; $P(\bar{B} \mid D)$ is the probability of non-occurrence of formation b, given the condition of being on a deposit; $P(\bar{B} \mid \bar{D})$ is the probability of non-occurrence of formation b, given the condition of not being on a deposit.

The absolute value of a weight indicates whether a criterion is slightly significant ($0<W<0.5$), significant ($0.5<W<1$), very significant ($1<W<2$), or discriminant ($W>2$). The contrast, C, which is the difference between the weights ($C=W^{+}-W^{-}$), is an overall measure of spatial association between the training points and the evidential theme, combining the effects of the two weights.

The spatial analysis is performed on the "deposits" and "geology" layers, using the Arc-SDM (Spatial Data Modeller) extension, developed for ArcView 3.x/Spatial Analyst ESRI® (Table 3).

3.3.2.2. Quantification of fault criterion and lithostratigraphic contact criterion. We used the algebraic method (Knox-Robinson and Groves, 1997) to quantify fault criteria and lithostratigraphic contact criteria. The objective is to determine a weighted density for the deposits (or quantity of metal) per unit of area (for lithostratigraphic formations), or per unit of length (for faults or lithostratigraphic contacts). The method is similar to that used for W^{+} in the WofE: identified relationships are quantified as in the weight of evidence technique, except that instead of calculating a probabilistic measure of prospectivity for areas of low and high prospectivity, a measure of deposit density is used (Knox-Robinson and Groves, 1997).

The favourability of faults and lithostratigraphic contacts was calculated by using the line favourability tool in the SynArc® software developed by BRGM (Braux, 1996). It is based on deposits (or occurrences), to which the same value 1 is assigned to indicate the presence of mineralization, whatever their size (the data regarding metal content being too fragmentary for use; see above). This tool allows a value based on a "points" layer (deposits) to be assigned to a linear object (faults or lithostratigraphic contacts). Placing a value on the line consists of looking for deposits located inside a band parallel to the line (Fig. 5). This band is defined by a minimum distance ($d_{\min}$) and a maximum distance ($d_{\max}$). A linear weighting is then performed: a value equal to 1 is given to any point located between the line and the minimum distance [100%]; a (linearly) decreasing value between 0 and 1 is given to any point lying between the minimum distance [100%] and the maximum distance [0%].

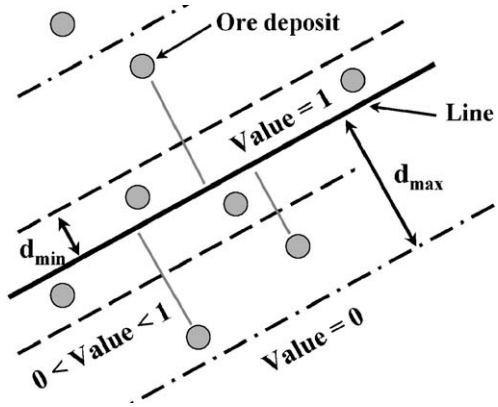

Fig. 5. Diagram illustrating line favourability tool in SynArc® software (Braux, 1996). Attribution of a value to a line (such as fault or lithostratigraphic contact) depends on distance of deposit from line.

The minimum distance used in this study is 1 km, whereas the maximum distance is 3 km, in accordance with the distances actually observed between deposits and faults (Fig. 6): ~50% of the deposits are at less than 1 km from a fault (maximum influence of the fault on the distribution of prospects), ~40% between 1 and 3 km (decreasing influence of the fault on the distribution of prospects), and 10% are beyond 3 km (no influence). Although the connection is less clearly defined for lithostratigraphic contacts, for the sake of uniformity the same distance parameters were used. Notice that the same deposit, for example one located near an intersection, may be included in several categories of faults or lithostratigraphic contacts.

Values were assigned to the "faults" criterion according to strike (using 10° class intervals, i.e., 0° to 10°, 10° to 20°, ... 170° to 180°). The weight (n_i) of fault category i, calculated from the line favourability, is equal to the sum of the weights of each of the faults belonging to this category. The calculated favourability, written Fav_i, is the relative index weight quotient (Pr_i=weight of each fault category, n_i, over the total weight of all the categories, N_{tot}), weighted by the relative length (Lr_i=length of family i, or Length_i, over the total length of all the faults in the area studied, $\mathrm{Length}_{\mathrm{tot}}$), (Eqs. (3), (4), (5), and Table 6).

$$\mathrm{Pr}_i = \frac{n_i}{N_{\mathrm{tot}}} \tag{3}$$

$$\mathrm{Lr}_i = \frac{\mathrm{Length}_i}{\mathrm{Length}_{\mathrm{tot}}} \tag{4}$$

$$\mathrm{Fav}_i = \ln\left(\frac{\mathrm{Pr}_i}{\mathrm{Lr}_i}\right). \tag{5}$$

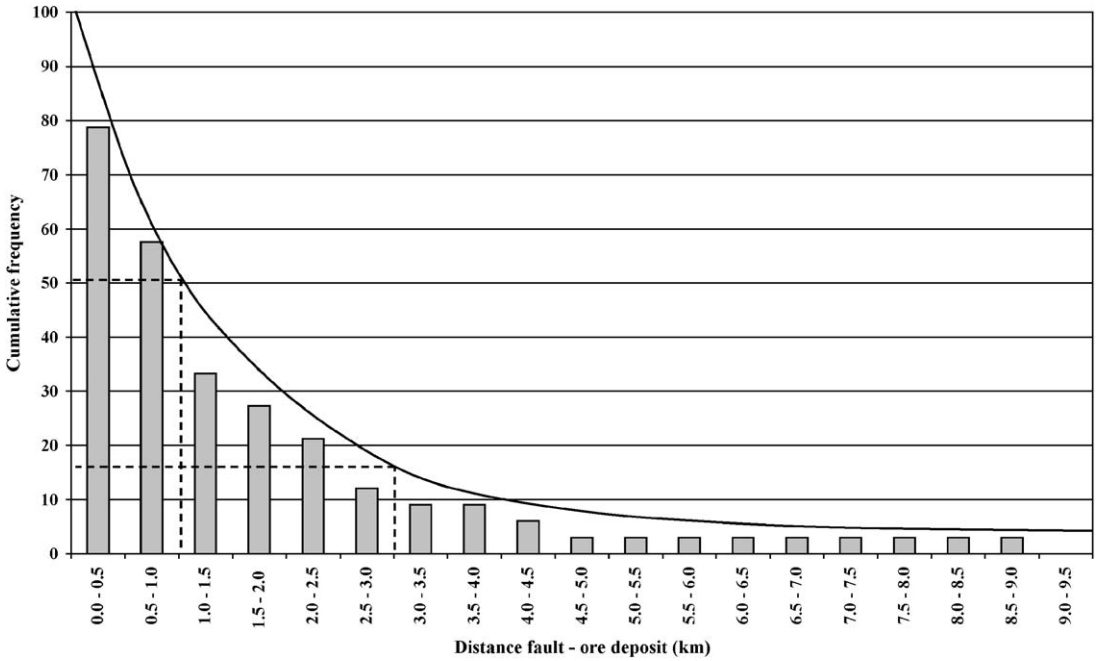

Fig. 6. Cumulative frequency of ore deposits as function of distance from nearest fault on 1:500,000 geological compilation.

The same procedure was applied for the "lithostratigraphic contacts" criterion. Each family of contacts is first identified by the two formations placed in contact. The weight (n_i) of a contact category i (e.g., Tp–Ts, Tp–Tp, etc.), calculated from the favourability of the line, is equal to the sum of the weights of each of the contacts belonging to this category. The calculated favourability, written Fav_i, is calculated in the same way as above.

For these two criteria, the ratio is greater than 1 for the most favourable families (Fav_i positive, in log value), and less than 1 for the least favourable families (Fav_i negative, in log value); see Eq. (5).

The results of the quantification of the fault and lithostratigraphic contacts criteria are shown in Tables 4 and 5, respectively.

Table 6
Algebraic method: calculation used for fault direction classes and lithostratigraphic contact classes

Class	Weight of class$_i$	Lengths of class$_i$
1	n_1	Length$_1$
:	:	:
5	n_5	Length$_5$
:	:	:
j	n_j	Length$_j$
	$N_{\mathrm{tot}} = \sum_{i=1}^{j} n_i$	$\mathrm{Length}_{\mathrm{tot}} = \sum_{i=1}^{j} \mathrm{Length}_i$

3.3.2.3. Geological structures criterion. At regional scale, two kinds of geological structures have been described in this part of NW Argentina: (i) the Tucumán and Desaguadero-Valle Fértil transfer zones (Fig. 1), and (ii) the Vicuña Pampa–Filo Colorado volcanic axis (Fig. 2). The precise nature of the transfer zones is debatable (Mon, 1976; de Urreiztieta, 1996; de Urreiztieta et al., 1996; Rossello, 2000). Toward their edges, the intensity of deformation decreases. Their quantification is therefore still subject to discussion. Nevertheless, their probable area of influence has been plotted on the compilation map.

3.3.3. Stage 3: development of the predictive map

The predictive map is a synthesis of the spatial association rules established and quantified during the preceding stages. Its objective is to produce a picture of the metallogenic potential of the area studied, in order to reach a better understanding of the factors that control the distribution of mineralization, and to trigger eventual exploration work in new areas. For the latter reason it is also called a prospectivity map (Knox-Robinson and Groves, 1997). In practice, this predictive map was obtained by adding up the various favourability scores for the three criteria defined during the preceding stages. In theory, it should enable the "rediscovery" of a high percentage of the known ore deposits, thus representing a kind of quality control for the method. However, its main interest is, of course, the

targeting of new areas for mineral exploration, i.e., areas with high favourability but without any known ore deposits or occurrences.

4. Predictive map: results and discussion

4.1. Results for favourability criteria

Lithostratigraphy Criterion (Table 3 and Fig. 7). The values of W^+ being fairly close to those of the contrast, C, these were the values finally selected. The area evaluated covers nearly 100,000 km^2. Of it, 50% are Quaternary sediments, 30% are basement, and the rest is essentially composed of Mesozoic rocks (~10%) and Tertiary sediments or volcanic rocks (~10%). The results obtained by using WofE show major differences between formations: the probability of having a deposit in the Tp formation is six times greater than in the Tvb formation. Intrusions of Tertiary age (Tp) are therefore clearly the most favourable formation. They carry 50% of the gold-bearing deposits, although they represent only 0.10% of the total area. The other favourable lithologies are Tertiary volcanic rocks (Tvb), Palaeozoic sedimentary formations (Pzs), Proterozoic–Palaeozoic metamorphic rocks (PePzm), and to a lesser degree Palaeozoic plutonic rocks (Pzp) and volcano-sedimentary deposits (Pzvs). The favourability of these basement formations is due to deposits that, at 1:500,000 scale, are still assigned to these polygons (e.g., Montey, Offir, El Oro), whereas the ore deposits are actually in or around Tertiary intrusions that do not crop out or are too small in size to be mapped at this scale. The other formations are unfavourable, or given as indeterminate by the method.

Faults Criterion (Table 4 and Fig. 8a, b). The favourability calculations, performed on fault trend, show four main groups. The most favourable ($Fav_i > 1$), are transverse structures, trending N060°–N070°E, N080°–N090°E, N100°–N110°E, and N120°–N130°E. Faults trending N070°–N080°E, N090°–N100°E, and N140°–N150°E appear slightly less favourable ($1 > Fav_i > 0.6$). These seven families seem to play a preponderant role in the distribution of gold, confirming previous studies at Andean scale (Hanuš et al., 2000), field observations at regional scale, and observations at the local scale at Bajo de la Alumbrera (Angera, 1999; Proffett, 2003), Agua Tapada (Alderete, 1999a), Agua Rica (Roco and Koukharsky, 1999), and La Mejicana (Mayón, 1999). Faults trending NE–SW appear only slightly favourable ($0.6 > Fav_i > 0$) despite their significance in terms of regional structure (de Urreiztieta, 1996).

Lithostratigraphic Contacts Criterion (Table 5 and Fig. 9). Four families of contacts can be distinguished. Two families of contacts are considered to be very favourable ($Fav_i > 4$), nine are favourable ($4 > Fav_i > 2$), 2), and eleven are slightly favourable ($2 > Fav_i > 0$). The

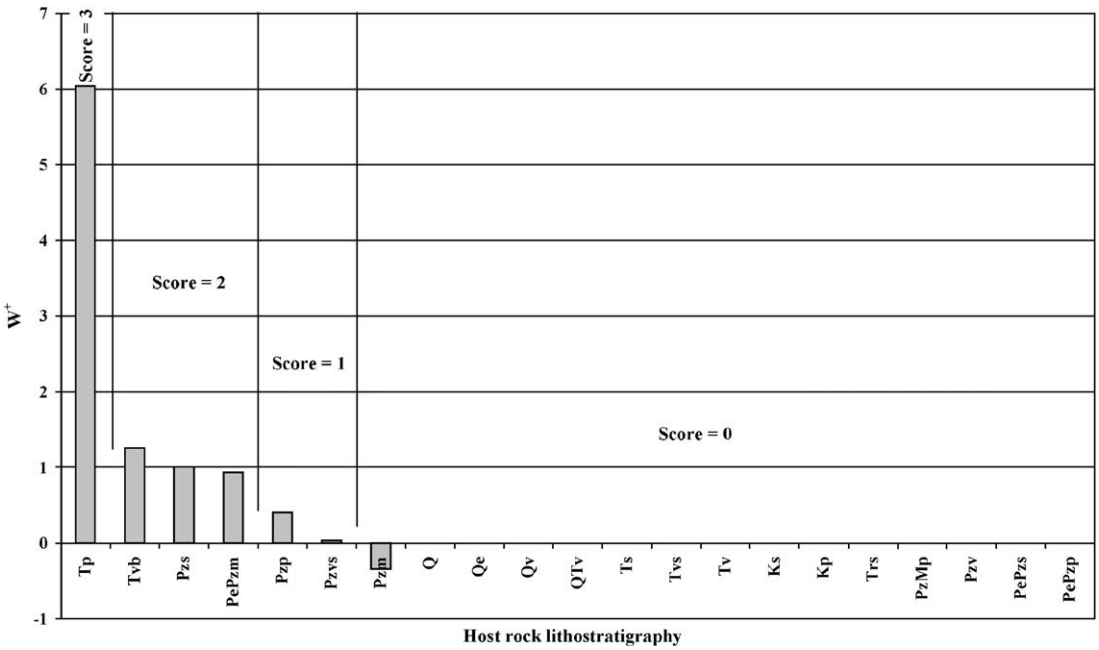

Fig. 7. Histogram showing results obtained by Weights of Evidence method (WofE—Bonham-Carter, 1994), for various lithologies cropping out in area studied. For lithostratigraphic units, see Appendix A.

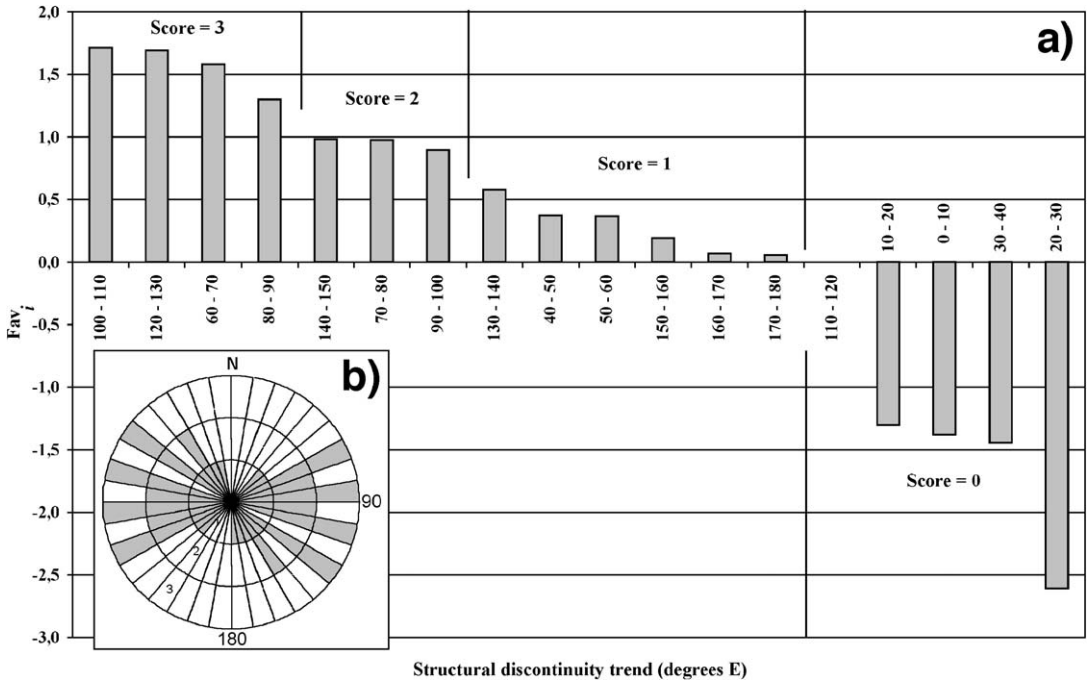

Fig. 8. (a) Favourability of fault trend classes, calculated by algebraic method (Knox-Robinson and Groves, 1997). (b) Rose diagram, showing favourability score assigned to each of class. Two families of favourable trends dominate, one nearly E–W, the other NW–SE.

other 13 appear unfavourable. Most of the favourable contacts are between Tertiary intrusions and other formations with favourable lithologies (e.g., Tvb, Pzs, PePzm, and Pzp), or to a lesser extent with formations having unfavourable lithologies (e.g., PePzs and Ts). The cumulative length of contacts whose calculated

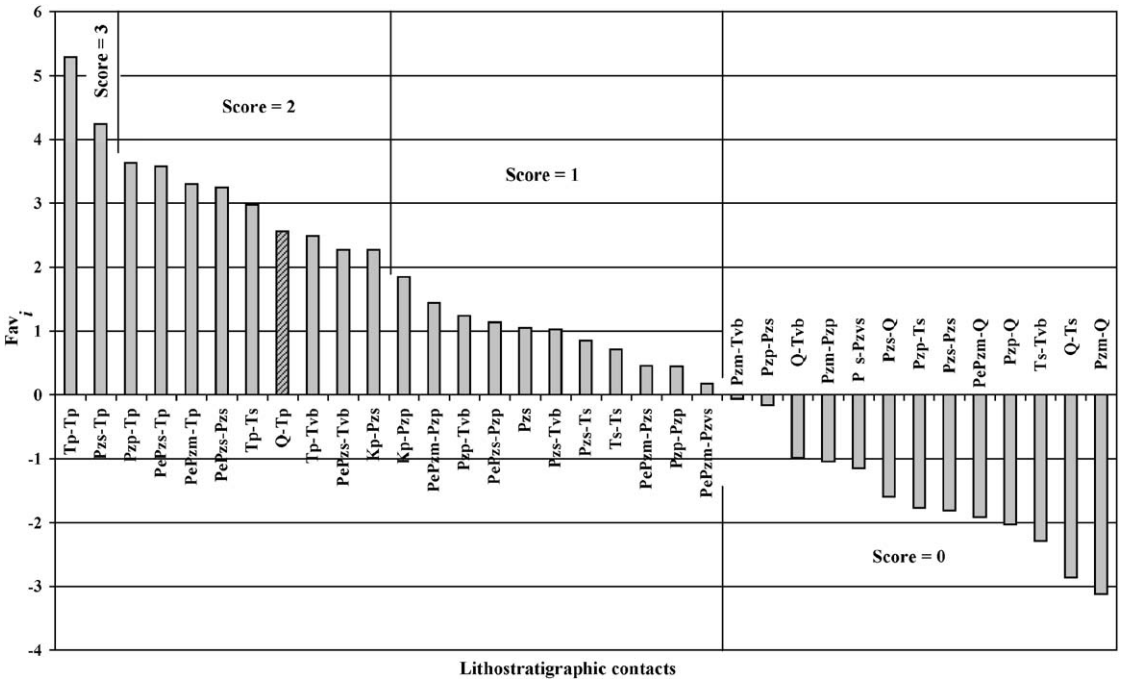

Fig. 9. Favourability of lithostratigraphic contact classes, calculated by algebraic method (Knox-Robinson and Groves, 1997). Q-Tp class (hatched) was given score of 0 (for explanation, see text). For lithostratigraphic units, see Appendix A.

favourability is greater than 2 (favourable to very favourable) is not great (~2.5% of the total length of lithostratigraphic contacts), so that the criterion is relatively selective and enables attention to be focussed on the areas that carry deposits.

4.2. Comments on the method

Four categories of score were identified for each of the criteria: very favourable = 3, favourable = 2, slightly favourable = 1, and unfavourable = 0 (Figs. 7, 8 and 9). This notation enables the same range of scores to be applied to all the criteria. The various criteria have therefore not been prioritized or weighted during processing.

Information on lithostratigraphy is used twice, once for country rock formations and once for contacts. Are these criteria independent (or redundant)? The lithostratigraphy of the country rock formations refers to chemical and petrochemical properties, whereas the contact between lithologies of different kinds involves the mechanical (physical) behaviour and rheological properties of the rocks. Though independence between these criteria may not be absolute, they nevertheless draw on separate properties.

The processing may sometimes create artefacts. It is essential to have an expert check these results, to confirm that they do not contradict field observations. For most of the criteria, the results seem to be correct, except for the Q-Tp category of the "lithostratigraphic contacts" criterion. For that category, the score was reduced to 0 (Table 5, category hatched in Fig. 9), in spite of its strong calculated favourability ($Fav_i = 2.98$), as these appears to represent a redundant artificial expression of the recent cover over the favourable Tp formation.

4.3. Comments on the predictive map

Superposition of the various criteria results in a predictivity map plotted on a scale that goes from 0 to 8, and not 9 as is theoretically possible (Fig. 10). The favourable groupings are relatively closely confined for values greater than 5; this score is one point above the mean, and resulting from the superposition of at least two favourable criteria.

The map shows 20 anomalous envelopes (1 to 20, Fig. 10). Some of these contain known deposits, whereas others do not. Some overlap with mining areas that are active (Bajo de la Alumbrera, Farallón Negro-Alto de la Blenda [envelope 1]), under development (Agua Rica [envelope 3]), or being explored and identified as prospects (Bajo San Lucas [envelope 2], Filo Colorado [envelope 3], Vicuña Pampa [envelope 5], and Cerro Azul [envelope 7]). On the other hand, others cover abandoned areas, suggesting that it would be useful to re-examine the data or do a more detailed study (Cerro Peinado [envelope 8], Mogote Rio Blanco [envelope 12], El Pararrayo [envelope 13], and La Mejicana [envelope 14]). Finally, some envelopes are in completely new areas (for example, 4, 6 to 11, and 15 to 20). The cutoff score value (favourability score ≥ 5) seems to be realistic: favourable areas are not too large, and their distribution is consistent with the structure of the area studied (70% of the known ore deposits are within the envelopes defined as favourable). Due to the above-mentioned exclusion of the favourable score for the Q-Tp lithostratigraphic contact, no favourable envelopes are taken across the Quaternary. This does not exclude the existence of hidden occurrences under the Quaternary cover, but is beyond the scope and limits of our approach.

At the southern edge of the Puna, favourable envelopes are about 30 km apart and they trend NW–SE (~N140°E) [envelopes 4 to 8; and, to a lesser extent, 1 and 2]. They mostly lie along the Vicuña Pampa–Filo Colorado volcanic axis, but seem to be somewhat offset in the SE. The work of Rossello (2000) suggests a genetic relationship between plutonic activity and mineralization around Vicuña Pampa (north of envelope 5) and Farallón Negro (envelope 1). To the south, near the Sierra de Famatina, two other anomalies [13 and 14] also trend NW–SE. At La Mejicana (Fig. 3a), the plutons hosting the mineralization were emplaced in structures trending NW–SE. They were later cut by post-mineralization fractures, trending N–S (Mayón, 1999).

Structures trending NE–SW enhance the favourability of certain areas, such as those south of Vicuña Pampa (envelope 5) and Farallón Negro (envelopes 1 and 2), as well as certain isolated areas in the Sierra de Velasco (envelope 16) and the Sierra de Ambato (envelope 19).

In the Sierra de Velasco, envelopes 16 to 18 are due to superposition of lithostratigraphy and fault criteria. However, these areas must be viewed with caution, because the tectonic structures here were interpreted from Landsat images (NASA, S-19-25, 2000). Envelopes 15 (south of the Sierra de Famatina) and 19 and 20 (in the Sierra de Ambato) appear more interesting, because favourability is due to the three main types of criteria, deduced from geological maps.

On the map, the position of the Tucumán Transfer Zone (Fig. 10) strengthens the interest of otherwise isolated areas (envelopes 9, 10, and 11). Likewise, the

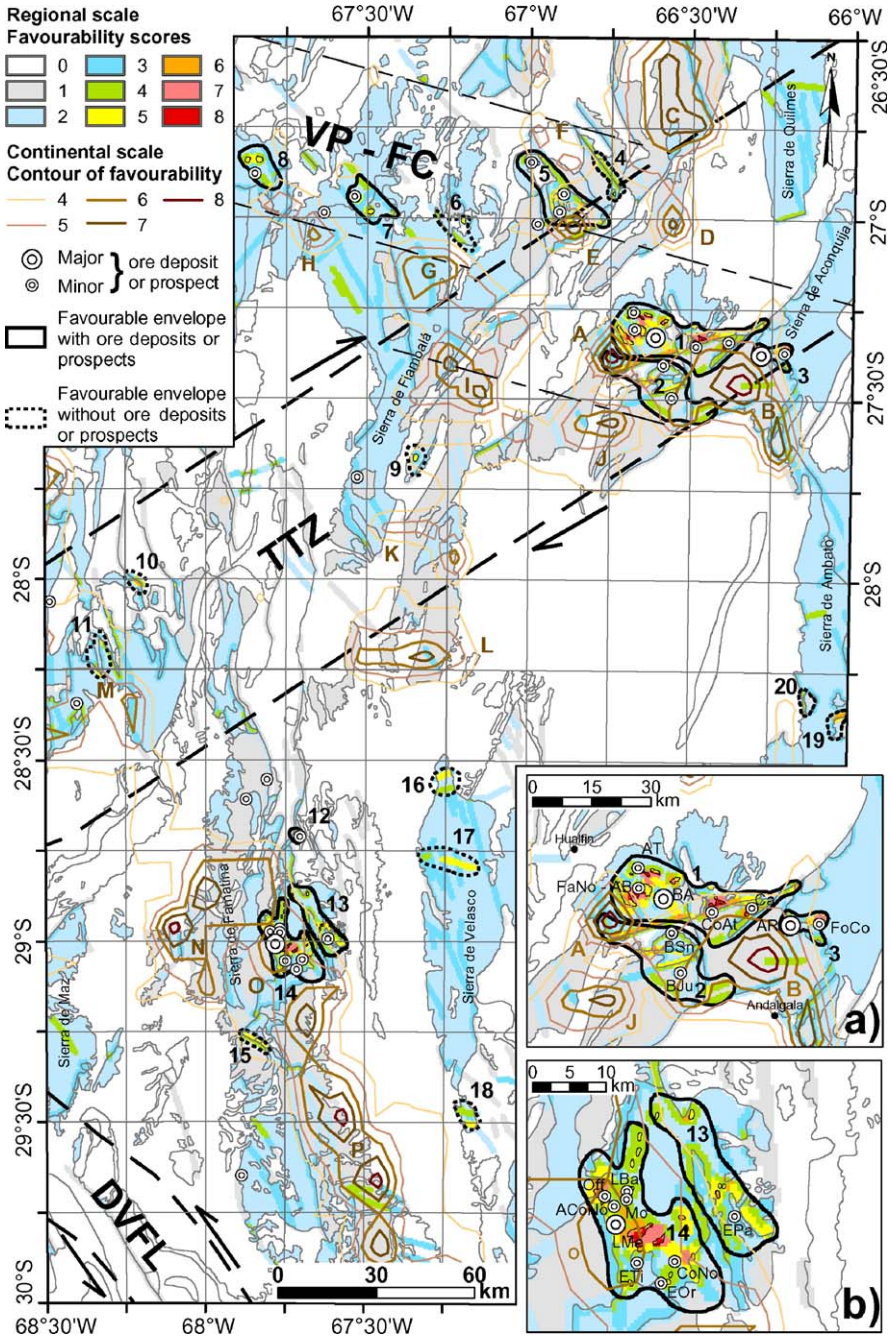

Fig. 10. Predictive map for gold in NW Argentina. The minimum width of the lineaments such as Tucumán Transfer Zone (TTZ) and Desaguadero-Valle Fértil Lineament (DVFL), as well as Vicuña Pampa–Filo Colorado magmatic axis (VP–FC), are indicated by the dashed lines enveloping these structures. Inset maps are for Farallón Negro Volcanic Complex (a) and Sierra de Famatina (b). For abbreviations, see Fig. 2. For targets 1 to 20 and targets A to P, see explanations in text.

Vicuña Pampa–Filo Colorado volcanic axis, considered to be favourable, gives added value to envelopes 1 to 8 and suggests that right-lateral displacement on the TTZ, during the Neogene, has offset the mineralized belt by about 40 km. Independently, restoration of fault heaves on a map, yields (i) horizontal displacements of at least 20 km along the TTZ, and (ii) clockwise rotations of fault blocks about vertical axes (de Urreiztieta, 1996; Gapais et al., 2000). Palaeomagnetic studies have yielded rotations of as much as 29° (Aubry et al., 1996).

According to Chernicoff et al. (2002), faults trending NE–SW cut older faults trending WNW–ESE in the vicinity of Farallón Negro.

5. Comparison of results from the continental- and regional-scale models

5.1. Methodological aspects: effects of a change in scale

Billa et al. (2004) did a multi-criteria study of Andean mineralization at continental scale (1:2,000,000). This was based on 113 gold orebodies and deposits of epithermal and porphyry type of Neogene age. To compare the results obtained at continental scale with those obtained at regional scale (1:500,000), we have plotted contours from the previous study (favourability score ≥ 4, i.e. 95% of the metal content) on the favourability map produced during the current study (Fig. 10).

On the 1:2,000,000 predictive map, the main districts (Farallón Negro, Agua Rica, and Famatina) were identified but mislocated by about 5 to 10 km (areas A, B, M, and O). New areas, such as Vicuña Pampa and its extension to the SE, were also identified (areas E and F) but mislocated. Because the mislocations were almost systematically to the SW, we believe that they mainly resulted from misinterpretation of projection systems on the original maps that were used for geological compilation. However, a lack of precision is not surprising, in view of the scale selected for the continental study and the corresponding pixel size (10×10 km).

At 1:2,000,000 (GIS Andes) some information becomes degraded, particularly when geological formations are of small surface area (for example, Tertiary porphyry stocks, which host the mineralization). During statistical processing, the deposit is assigned to a country rock polygon, which may thereby acquire an exaggerated favourability. This bias becomes smaller or non-existent at 1:500,000, because most of the Tertiary intrusions could then be mapped in detail and the deposits were georeferenced with greater accuracy. This explains why a certain number of areas that were favourable at the continental scale were not confirmed at the regional scale (e.g., areas C, D, I, J, K, L, N, and P). Although the basement formations still retain some favourability, it is less significant.

New anomalous areas were delimited at 1:500,000, particularly envelopes 9, 10, and 11 (along the Tucumán Transfer Zone), 15 (south of Sierra de Famatina), 16 to 18 (Sierra de Velasco), and 19 and 20 (Sierra de Ambato). These studies also led to new ideas about the spatial distribution of mineralized areas, for example, favourable envelopes develop along fault corridors trending E–W or NW–SE (Fig. 10), and lie on a volcano-magmatic axis.

The regional-scale work has allowed us (1) to easily recognize the mineralized areas, (2) to identify new targets or to re-identify occurrences that had not been included in the data calculation, and (3) given the accuracy (precision) of the information, to define better certain metallotects, such as the preferred directions of emplacement of mineralization. The processing procedure seems well suited to identifying areas of interest at regional scale (over areas of 100 to 300 km^2). On the other hand, the continental-scale work, although it is less detailed and more general in nature, is still efficient for identifying targets of larger size (on the order of 300 to 1000 km^2). It identified the main deposits and targets such as Vicuña Pampa, which has been confirmed independently by field studies (Rossello, 1980, in press). However, the lack of detail, which is inherent to mapping at 1:2,000,000, results in favourabilites that may be fictitious and may dominate parts of the predictive map. The tool, therefore, remains best suited to defining areas of interest at the strategic level.

5.2. Metallogenetic aspects: effects of the jump in scale and of structural knowledge of the region

At regional scale, more details can be included. Good examples are structural data (de Urreiztieta, 1996; de Urreiztieta et al., 1996; Fig. 4b). The metallotects described in the preceding paragraphs seem to be controlled by the orientations of certain structural features. Moreover, a compilation of the chronology of mineralizing events during the Neogene (see Table 2) shows that the emplacement of the mineral occurrences is (i) later than a magmatic phase; and (ii) earlier than or synchronous with a phase of compressional tectonics. In NW Argentina, two different situations for the emplacement of mineralization can be distinguished, one typical of the northern part (Vicuña Pampa and Farallón Negro), the other of the southern part (Sierra de Famatina).

In the north, the Tucumán Transfer Zone appears to offset the Vicuña Pampa–Filo Colorado magmatic axis (Fig. 11a). In the known ore deposits, mineralized veins and Neogene andesitic dykes trend mainly N125°E to N150°E (Proffett, 2003). This is particularly true for the Farallón Negro-Alto de la Blenda mine (Fig. 11b), where the veins reach maximal thickness when they have such trends (Alderete, 1999c). Around Bajo de la

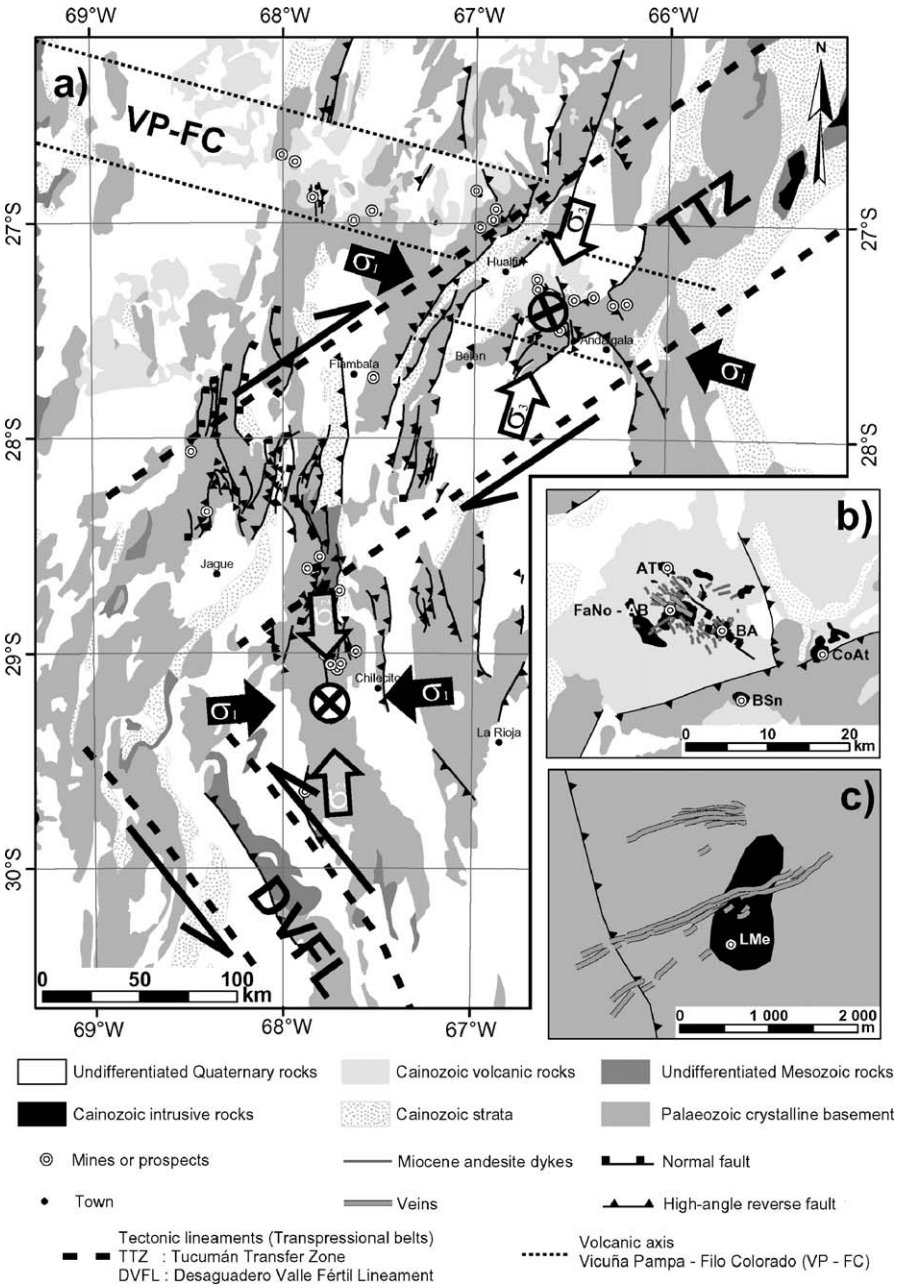

Fig. 11. Control of inferred principal stress on emplacement of mineralization in NW Argentina. Right-lateral Tucumán transpressional zone (TTZ) and left-lateral Desaguadero-Valle Fértil transpressional zone (DVFL) are conjugate structures (after Rossello et al., 1996b). A regional consequence of the TTZ is the offset of the Vicuña Pampa–Filo Colorado magmatic axis (VP–FC) by about 40 km. Inset maps show andesitic dykes and veins in Farallón Negro Volcanic Complex (b; after Proffett, 2003), and mineralized veins at La Mejicana mine, Sierra de Famatina (c; after Brodtkorb and Schalamuk, 1999). Broad arrows indicate principal stresses, σ_1 (black), σ_2 (grey) and σ_3 (white).

Alumbrera mine, Rossello et al. (1996a) attributed the elliptical shape and spatial arrangement of outcrops to Neogene deformation within the TTZ. Transverse faults, striking ~N145°E, appear to have controlled Miocene–Pliocene sub-volcanic intrusions and they in turn are associated with the main mineral deposits (Rossello, 2000). The transverse faults have left-lateral components and are conjugate to the right-lateral faults of the TTZ. The mineralization is in dilational zones, which are close in orientation to the inferred greatest principal stress (compression), as might be expected for hydraulic fracturing (Fig. 11a). The principal stress

direction would appear to be controlled, partly by the topographic effect of the Puna and partly be right-lateral transpression in the TTZ (Fig. 4a and b).

In the south, the mineralization at La Mejicana mine is in veins striking N070°E to N080°E (Fig. 11c; Brodtkorb and Schalamuk, 1999). It was controlled by Pliocene intrusive bodies channelled by NW–SE structures (Mayón, 1999). This strike (~N080°E) is superimposed on that of the E–W to WSW–ENE axes of shortening obtained from a kinematic study of the faults (de Urreiztieta et al., 1996), and is in agreement with the direction of convergence between the Nazca and South American Plates (Fig. 1; Pardo-Casas and Molnar, 1987; Somoza, 1998). The Sierra de Famatina (SF) trends N–S, between two major transpressional tectonic structures, the TTZ and the DVFL. The latter is bounded on the east and west by high-angle reverse faults. The uplift of this range as a "pop-up" structure implies crustal thickening (Ramos et al., 2002). It may also have occurred under constriction (Rossello et al., 1996b), so that the principal stresses σ_1 and σ_2 were sub-horizontal and had similar values ($\sigma_1 \geq \sigma_2 > \sigma_3$). This state of stress would be propicious to the development of a laccolith at depth, its surface expression being the large hydrothermal alteration halo seen at La Mejicana. If the reverse faults that bound the Sierra de Velasco (SV) on the east reached an equivalent depth under the Sierra de Famatina, the source magma might have escaped towards the east. This could explain the favourable areas (anomalies 16 to 18, Fig. 10) that appeared during multi-criteria processing (see above). The hypothesis, whereby mineralization and hydrothermal activity are due to a laccolith, warrants more detailed study in the Sierras Pampeanas and a comparison with similar systems elsewhere, e.g., Baia Mare in Romania (Crahmaliuc and Crahmaliuc, 1997; Bailly et al., 1997).

To both north and south, the mineralization is along a network of veins and veinlets, which appear to have formed in orientations sub-parallel to the principal stress σ_1 and perpendicular to the minimum stress σ_3, as obtained experimentally for hydraulic fractures (Hubbert and Willis, 1957).

6. Conclusions

A multi-criteria predictive study for gold in NW Argentina, conducted at 1:500,000, has recognized mining areas that are active (e.g., Bajo de la Alumbrera), under development (e.g. Agua Rica), or abandoned (e.g., La Mejicana), and has identified new targets (e.g., Vicuña Pampa). The predictive map was compiled from data acquired in the field, and data available in the literature (e.g., geological maps) or included in the GIS Andes database (BRGM, 2001). Production of a predictive map requires a homogeneous population of deposits, likely to have been controlled by an identical set of factors: the same commodity, the same metallogenetic period, and the same ore-forming processes. The change of scale (from continental to regional) obviously leads to greater precision. However, the reduction in area is accompanied by a corresponding decrease in the number of available ore deposits for the calculation and learning phases, and their descriptions are no more detailed. A population that contains relatively few deposits, and whose associated data are not always homogeneous, makes interpretation difficult. The validity of the results must be confirmed by an expert in the field: hence the use of an "expert-guided data-driven" approach. Moreover, this reduction in scale invalidates the use of some of the information layers. This is especially true of geodynamics-related criteria (depth and dip of the subducted plate) and of the "regional structures" criterion. At regional scale, the depth and dip of the subducted plate do not vary significantly, and "regional structures", as a criterion, is too vague and poorly constrained. On the other hand, at this scale a more precise knowledge of the structural context has led to better understanding of the principles governing the distribution of deposits.

According to structural and kinematic analyses, the direction of shortening was (1) E–W in the Sierra de Famatina, as a result of plate convergence and (2) NW–SE in the Farallón Negro district, due to the combined effects of topography and right-lateral faulting in the TTZ at the southern edge of the Puna. The orientations of the veins in the deposits coincide with these two directions. In situations of this kind, the mineralization is emplaced in dilational fractures, sub-perpendicular to the least principal stress.

The continental-scale GIS is particularly suited for use at the strategic scale of country, craton, or orogen. The suggested upper limit of use of GISs for mineral potential mapping, placed at 1:500,000 scale by Knox-Robinson and Groves (1997), may therefore be extended to 1:2,000,000 (Lips et al., 2002). As we have seen, the effectiveness of these systems will then greatly depend on the quality of their application and on detailed checking of the data. Ignoring the projection system of any map used in a compilation (a frequent occurrence) may lead to significant errors, which may not be easy to detect. On the other hand, a regional-scale GIS, which by its nature draws on much more detailed data, will enable a better understanding of the roles of the various metallotects, and the identification of more varied targets. A system of this type, therefore,

is particularly suited to tactical exploration, over limited areas.

Acknowledgments

The authors want to thank Dr. Luis F. Navarro García for his help in organizing the field trip and Dr. Juan Angera for his welcome on the Bajo de la Alumbrera mine site. Reviews by Drs. Carl Knox-Robinson and Miguel Gallardo and editorial comments by Alexander Yakubchuk contributed to significantly improve the manuscript and are acknowledged. GIS Andes was developed as a part of two BRGM R&D projects, "Andean Metallogeny" and "Global Environmental and Metallogenic Syntheses" (GEMS). This is BRGM contribution No. 3482.

Appendix A. Lithostratigraphic units and their abbreviations

Q = Undifferentiated Quaternary; Qe = Quaternary salar evaporite deposits; Qv = Undifferentiated Quaternary arc volcanic rocks; Ts = Undifferentiated Tertiary marine and continental deposits; Tv = Undifferentiated Tertiary volcanic rocks; Tp = Undifferentiated Tertiary plutonic rocks; Tvs = Undifferentiated Tertiary volcano-sedimentary deposits; Tvb = Tertiary basaltic volcanic rocks; Ks = Undifferentiated Cretaceous marine and continental deposits; Kp = Undifferentiated Cretaceous plutonic rocks; Trs = Undifferentiated Triassic marine and continental deposits; Pz–Mz = Undifferentiated Palaeozoic–Mesozoic rocks; Pzs = Undifferentiated Palaeozoic marine and continental deposits; Pzvs = Palaeozoic volcano-sedimentary deposits; Pzv = Undifferentiated Palaeozoic volcanites; Pzp = Undifferentiated Palaeozoic plutonic rocks; Pzm = Undifferentiated Palaeozoic metamorphic rocks; PePzs = Undifferentiated Proterozoic and Palaeozoic marine and continental deposits; PePzp = Undifferentiated Proterozoic and Palaeozoic plutonic rocks; PePzm = Undifferentiated Proterozoic and Palaeozoic metamorphic rocks.

References

Alderete, M., 1999a. Bajo de Agua Tapada, Catamarca. In: Zappettini, E.O. (Ed.), Recursos Minerales de la República Argentina, Instituto de Geología y Recursos Minerales SEGEMAR (Buenos Aires), Anales, vol. 35, pp. 1475–1478.

Alderete, M., 1999b. Bajo de San Lucas, Catamarca. In: Zappettini, E.O. (Ed.), Recursos Minerales de la República Argentina. Instituto de Geología y Recursos Minerales SEGEMAR (Buenos Aires), Anales, vol. 35, pp. 1471–1473.

Alderete, M., 1999c. Distrito Farallón Negro-Alto de la Blenda, Catamarca. In: Zappettini, E.O. (Ed.), Recursos Minerales de la República Argentina, Instituto de Geología y Recursos Minerales SEGEMAR (Buenos Aires), Anales, vol. 35, pp. 1637–1642.

Allmendinger, R.W., Jordan, T.E., Kay, S.M., Isacks, B.L., 1997. The evolution of the Altiplano-Puna Plateau of the Central Andes. Annual Reviews of Earth and Planetary Science 25, 139–174.

Angera, J., 1999. Mina Bajo de la Alumbrera, Catamarca. In: Zappettini, E.O. (Ed.), Recursos Minerales de la República Argentina, Instituto de Geología y Recursos Minerales SEGEMAR (Buenos Aires), Anales, vol. 35, pp. 1451–1461.

Assumpção, M., Araujo, M., 1993. Effect of the Altiplano-Puna plateau, South America, on the regional intraplate stress. Tectonophysics 221, 475–496.

Aubry, L., Roperch, P., de Urreiztieta, M., Rossello, E.A., Chauvin, A., 1996. Paleomagnetic study along the southeastern edge of the Altiplano–Puna Plateau: Neogene tectonic rotations. Journal of Geophysical Research 101, 17,883–17,899.

Avila, J., Lazarte, J.E., Gianfrancisco, M., Fogliata, A.S., 1999a. Distrito aurifero Culampajá, Catamarca. In: Zappettini, E.O. (Ed.), Recursos Minerales de la República Argentina, Instituto de Geología y Recursos Minerales SEGEMAR (Buenos Aires), Anales, vol. 35, pp. 557–562.

Avila, J., Lazarte, J.E., Gianfrancisco, M., Fogliata, A.S., 1999b. Metalogénesis de wolframio y estaño de Catamarca. In: Zappettini, E.O. (Ed.), Recursos Minerales de la República Argentina, Instituto de Geología y Recursos Minerales SEGEMAR (Buenos Aires), Anales, vol. 35, pp. 563–573.

Bailly, L., Milesi, J.-P., Leroy, J., Marcoux, E., 1997. Les minéralisations épithermales de Baia Mare (Nord Roumanie): nouvelles données minéralogiques et microthermométriques. Comptes Rendus de l'Académie des Sciences, Paris 327 (II), 385–390.

Billa, M., Cassard, D., Guillou-Frottier, L., Lips, A.L.W., Tourlière, B., 2002. Assessment of GIS Andes: predictive mapping of Neogene gold-bearing magmatic-hydrothermal systems in the Central Andes. Fifth International Symposium on Andean Geodynamics, September 16–18, 2002, Toulouse, France, IRD Publ., Paris, pp. 89–92. Extended Abstracts Volume.

Billa, M., Cassard, D., Lips, A.L.W., Bouchot, V., Tourlière, B., Stein, G., Guillou-Frottier, L., 2004. Predicting gold-rich epithermal and porphyry system in the central Andes with a continental-scale metallogenic GIS. Ore Geology Reviews 25, 39–67.

Bonham-Carter, G.F., 1994. Geographic information systems for geoscientists. Modelling with GIS Computer Methods in the Geosciences, vol. 13. Pergamon, New York. 398 pp.

Bonham-Carter, G.F., Agterberg, F.P., Wright, D.F., 1989. Weights of evidence modeling: a new approach to mapping mineral potential. In: Agterberg, F.P., Bonham-Carter, G.F. (Eds.), Statistical Applications in Earth Sciences, Geological Survey of Canada, vol. 89-9, pp. 171–183.

Boudesseul, N., de Bremond d'Ars, J., Cobbold, P.R., Gapais, D., Hallot, E., 1999. Relationships between Cenozoic volcanism and tectonics in Central Andes. European Union of Geosciences (EUG X), March 28–April 1, Strasbourg, France, p. 834. Abstracts Volume.

Bougrain, L., Bouchot, V., Cassard, D., Lips, A.L.W, Gonzalez, M., Stein, G., Alexandre, F., 2003. Knowledge recovery for continent-scale metal exploration by neural networks. Natural Resources Research 12-3, 173–181.

Braux, C., 1996. Cartographie multicritère: guide technique. Unpubl. BRGM Report R-39146, Orléans, France. 71 pp.

BRGM, 2001. GIS Andes: The Geological Information System for the Andes. Georama Andes version 2.0., CD-ROM, BRGM Editor, France.

Brodtkorb, M., Schalamuk, B., 1999. Yacimientos de cobre y oro de la Sierra de Famatina, La Rioja. In: Zappettini, E.O. (Ed.), Recursos Minerales de la República Argentina Instituto de Geología y Recursos Minerales SEGEMAR (Buenos Aires), Anales, vol. 35, pp. 1659–1663.

Brown, W.M., Gedeon, T.D., Groves, D.I., Barnes, G., 2000. Artificial neural networks: a new method for mineral prospectivity mapping. Australian Journal of Earth Sciences 47, 757–770.

Burrough, P.A., McDonnell, R.A., 1998. Principles of Geographic Information Systems. Oxford University Press. 333 pp.

Cahill, T., Isacks, B.L., 1992. Seismicity and the shape of the subducted Nazca plate. Journal of Geophysical Research 97, 17,503–17,529.

Cassard, D., 1999a. GIS ANDES: a metallogenic GIS of the Andes Cordillera. Fourth International Symposium on Andean Geodynamics, October 4–6, 1999, Göttingen, Germany, IRD Publ., Paris, pp. 147–150. Extended Abstracts Volume.

Cassard, D., 1999b. GIS Andes on the Web: http://www.brgm.fr/sigandes/.

Cassard, D., Billa, M., Bouchot, V., Salleb, A., Stein, G., Tourlière, B., 2001. Predictive mapping with GIS Andes datasets. European Union of Geosciences (EUG XI), April 8–12, Strasbourg, France, p. 265. Abstracts Volume.

Cassard, D., Lips, A.L.W., Itard, Y., Stein, G., 2003. GIS Central Europe: an operational tool to improve metallogenic thinking, support exploration activities and contribute to the sustainability of the mining industry. Seventh Biennal SGA Meeting "Mineral Exploration and Sustainable Development", Athens, Greece, August 24–28, 2003, Extended Abstracts Volume.

Cassard, D., Lips, A.L.W., Leistel, J.M., Itard, Y., Debeglia, N., Guillou-Frottier, L., Spakman, W., Stein, G., Husson, Y., 2004. Understanding and assessing European mineral resources—a new approach using GIS Central Europe. Schweizerische Mineralogische und Petrographische Mitteilungen 84, 3–24.

Castaing, C., Cassard, D., Gros, Y., Moisy, M., Chabod, J.C., 1993. Role of rheological heterogeneities in vein-ore localization. Canadian Journal of Earth Sciences 30, 113–123.

Chernicoff, C.J., Richards, J.P., Zappettini, E.O., 2002. Crustal lineament control on magmatism and mineralization in northwestern Argentina: geological, geophysical, and remote sensing evidence. Ore Geology Reviews 21, 127–155.

Coughlin, T.J., O'Sullivan, P.B., Kohn, B.P., Holcombe, R.J., 1998. Apatite fission-track thermochronology of the Sierras Pampeanas, central western Argentina: implications for the mechanism of plateau uplift in the Andes. Geology 26, 999–1002.

Coutand, I., Cobbold, P.R., de Urreiztieta, M., Gautier, P., Chauvin, A., Gapais, D., Rossello, E.A., 2001. Style and history of Andean deformation, Puna plateau, northern Argentina. Tectonics 20, 210–234.

Crahmaliuc, R., Crahmaliuc, A., 1997. Caractéristiques structurales et métallogénétiques des roches magmatiques néogènes de Baia Sprie-Est, à l'aide de la modélisation magnétique en deux dimensions. Romanian Journal of Mineral Deposits 78, 47–52.

de Urreiztieta, M., 1996. Tectonique néogène et bassins transpressifs en bordure méridionale de l'Altiplano-Puna (27°S), Nord-Ouest argentin. Mémoires de Géosciences-Rennes 72. 311 pp.

de Urreiztieta, M., Gapais, D., Le Corre, C., Cobbold, P.R., Rossello, E.A., 1996. Cenozoic dextral transpression and basin development at the southern edge of the Altiplano–Puna, northwestern Argentina. Tectonophysics 254, 17–39.

Gapais, D., Cobbold, P.R., Bourgeois, O., Rouby, D., Urreiztieta, M.de., 2000. Tectonic significance of fault-slip data. Journal of Structural Geology 22, 881–888.

Garcia, H., Rossello, E., 1984. Geología y yacimientos minerales de Papachacra, departamento de Belén, Provincia de Catamarca. Noveno Congreso Geológico Argentino, San Carlos de Bariloche. Actas VII, 245–259.

Gemuts, I., Little, M.L., Giudici, J., 1996. Precious and base metal deposits in Argentina. SEG Newsletter 25, 7–13.

Godeas, M., Cardo, R., Carrizo, R., Cruz Zuloeta, G., Gonzáles, R., Korzeniewski, L.I., Lopez, H., Mallimacci, H., Martinez, L., Ramallo, E., Valladares, H., Zubia, M., 1999. Inventario de yacimientos y manifestaciones de minerales metalíferos e industriales de la República Argentina. In: Zappettini, E.O. (Ed.), Recursos Minerales de la República Argentina, Instituto de Geología y Recursos Minerales SEGEMAR (Buenos Aires), Anales, vol. 35, pp. 1979–2172.

González Bonorino, F., 1947. Carta Geológico-Económica de la República Argentina, Hojas 12d (Capillitas) y 13d (Andalgalá), escala 1:200.000. Dirección General de Minas y Geología de Argentina, Buenos Aires.

González, O., Barber, E., Aceñolaza, F., Toselli, A., Durand, F., 1994. Mapa geológico de la Provincia de Tucumán, escala 1:500.000. Secretaría de Minería, Dirección Nacional del Servicio Geológico de Argentina, Buenos Aires.

Guerrero, M., Lavandaio, E., Marcos, O., Caminos, R., Nullo, F., Panza, J., Fernandez, J., Reinoso, M., 1993. Mapa geológico de la Provincia de La Rioja, escala 1:500.000. Secretaría de Minería. Dirección Nacional del Servicio Geológico de Argentina, Buenos Aires.

Guillou, J., 1999. El pórfido cuprifero Filo Colorado, Catamarca. In: Zappettini, E.O. (Ed.), Recursos Minerales de la República Argentina. Instituto de Geología y Recursos Minerales SEGEMAR (Buenos Aires), Anales, vol. 35, pp. 1493–1494.

Hanuš, V., Vaněk, J., Špičák, A., 2000. Seismically active fracture zones and distribution of large accumulations of metals in the central part of Andean South America. Mineralium Deposita 35, 2–20.

Hubbert, M.K., Willis, D.G., 1957. Mechanics of hydraulic fracturing. Petroleum Transactions of the American Institute of Mining Engineers 210, 153–168.

Isacks, B.L., 1988. Uplift of the central Andean plateau and bending of the Bolivian orocline. Journal of Geophysical Research 93, 3211–3231.

Jordan, T.E., Allmendinger, R.W., 1986. The Sierras Pampeanas of Argentina: a modern analogue of Rocky Mountain foreland deformation. American Journal of Science 286, 737–764.

Jordan, T.E., Isacks, B.L., Ramos, V.A., Allmendinger, R.W., 1983. Mountain building in the Central Andes. Episodes 1983 (3), 20–26.

Kay, S.M., Mpodozis, C., 2002. Magmatism as a probe to the Neogene shallowing of the Nazca plate beneath the modern Chilean flat-slab. Journal of South American Earth Sciences 15, 39–57.

Kay, S.M., Mpodozis, C., Coira, B., 1999. Magmatism, tectonism, and mineral deposits of the Central Andes (22°–33°S latitude). In: Skinner, B.J (Ed.), Geology and Ore Deposits of the Central Andes, vol. 7. SEG Special Publication, pp. 27–59.

Kemp, L.D., Bonham-Carter, G.F., Raines, G.L., Looney, C.G., 2001. Arc-SDM: ArcView extension for spatial data modelling using weights of evidence, logistic regression, fuzzy logic and neural network analysis. http://ntserv.gis.nrcan.gc.ca/sdm/.

Kley, J., Monaldi, C.R., Salfity, J.A., 1999. Along-strike segmentation of the Andean foreland: causes and consequences. Tectonophysics 301, 75–94.

Knox-Robinson, C.M., Groves, D.I., 1997. Gold prospectivity mapping using a Geographic Information System (GIS) with examples from the Yilgarn Block of Western Australia. Chronique de la Recherche Minière 529, 127–138.

Lapidus, A., Padula, V., 1982. Exploración de la Mina King Tut, provincia de la Rioja. Evaluación de resultados. Estudios Mineros Integrales SRL, unpublished report.

Lips, A.L.W., Cassard, D., Bouchot, V., Billa, M., Salleb, A., Gonzalez, M., Bougrain, L., Vrain, C., Tourlière, B., Stein, G., Alexandre, F., 2002. Quantitative assessments of a continent-scale metallogenic GIS by data-driven and knowledge-driven approaches to construct decision-aid documents. GIS in Geology International Conference, Vernadsky SGM RAS, November 13–15, 2002, Moscow, pp. 74–76. Extended Abstracts Volume.

Losada-Calderón, A.J., Mc Bride, S.L., Bloom, M.S., 1994. The geology and $^{40}Ar/^{39}Ar$ geochronology of magmatic activity and related mineralization in the Nevados del Famatina mining district, La Rioja province, Argentina. Journal of South American Earth Sciences 7, 9–24.

Marques, F.O., Cobbold, P.R., 2002. Topography as a major factor in the development of arcuate thrust belts: insights from sandbox experiments. Tectonophysics 348, 247–268.

Marquez-Zavalia, M., 1999. Del yacimiento Capillitas, Catamarca. In: Zappettini, E.O. (Ed.), Recursos Minerales de la República Argentina, Instituto de Geología y Recursos Minerales SEGEMAR (Buenos Aires), Anales, vol. 35, pp. 1643–1652.

Martínez, L., Nullo, F., Caminos, R., Panza, J., Chipulina, M., Zappettini, E., 1995. Mapa geológico de la Provincia de Catamarca, escala 1:500.000. Secretaría de Minería, Dirección Nacional del Servicio Geológico de Argentina.

Matteini, M., Mazzuoli, R., Omarini, R., Cas, R., Maas, R., 2002. Geodynamical evolution of Central Andes at 24°S as inferred by magma composition along the Calama–Olacapato–El Toro transversal volcanic belt. Journal of Volcanology and Geothermal Research 118, 205–228.

Mayón, C., 1999. Depósitos de molibdeno y cobre diseminados en la Sierra de Famatina, La Rioja. In: Zappettini, E.O. (Ed.), Recursos Minerales de la República Argentina, Instituto de Geología y Recursos Minerales SEGEMAR (Buenos Aires), Anales, vol. 35, pp. 1495–1505.

McBride, S.L., 1972. A potassium–argon age investigation of igneous and metamorphic rocks from Catamarca and La Rioja provinces, Argentina: unpublished MSc dissertation, Kingston, Ontario, Queen's University, 101 pp.

Mon, R., 1976. La tectonica del borde oriental de los Andes en las Provincias de Salta, Tucumán y Catamarca, Republica Argentina. Asociacion Geológica Argentina, Revista 31, 65–72.

Nelson, E., 1996. Suprasubduction mineralization: metallo-tectonic terranes of the Southernmost Andes. American Geophysical, 315–329.

NASA, 2000. Landsat 7 TM image, S-19-25_2000.

Oyarzún, J., 2000. Andean metallogenesis. A synoptical review and interpretation. In: Cordani, U.G., Milani, E.J., Thomaz Filho, A., Campos, D.A. (Eds.), Tectonic Evolution of South America. 31st International Geological Congress, Rio de Janeiro, Brazil, August 6–17, pp. 725–753.

Pardo-Casas, F., Molnar, P., 1987. Relative motion of the Nazca (Farallón) and South American plates since late Cretaceous time. Tectonics 6, 233–248.

Parent, C., Spaccapietra, S., Zimanyi, E., 2000. MurMur: database management of multiple representations. AAAI-2000 Workshop on Spatial and Temporal Granularity, Austin, Texas, July 30, 2000.

Passarello, J., Romero, H., Navarro, J., 1992. Grupo minero El Oro, La Rioja, Dirreción Provincial de Mineria, unpublished report.

Peralta, E., 1999. Distrito aurifero de Cerro Atajo, Catamarca. In: Zappettini, E.O. (Ed.), Recursos Minerales de la República Argentina. Instituto de Geología y Recursos Minerales SEGEMAR (Buenos Aires), Anales, vol. 35, pp. 1653–1657.

Proffett, J.M., 2003. Geology of the Bajo de la Alumbrera porphyry copper–gold deposit, Argentina. Economic Geology 98, 1535–1574.

Ramos, V.A., 1999. Ciclos orogénicos y evolución tectonica. In: Zappettini, E.O. (Ed.), Recursos Minerales de la República Argentina, Instituto de Geología y Recursos Minerales SEGEMAR (Buenos Aires), Anales, vol. 35, pp. 29–49.

Ramos, V.A., Cristallini, E.O., Perez, D., 2002. The Pampean flat-slab of the Central Andes. Journal of South American Earth Sciences 15, 59–78.

Ricci, H.I., Valladores Carrillo, H., Pezzutti, N., Godeas, M., Segal, S.J., 1999. Distrito Minero La Hoyada, Catamarca. In: Zappettini, E.O. (Ed.), Recursos Minerales de la República Argentina, Instituto de Geología y Recursos Minerales SEGEMAR (Buenos Aires), Anales, vol. 35, pp. 1627–1636.

Richards, J.P., 2003. Tectono-magmatic precursors for porphyry Cu–(Mo–Au) deposit formation. Economic Geology 98, 1515–1533.

Roco, R., Koukharsky, M., 1999. El pórfiro cupro-molibdenifero Agua Rica y las manifestaciones epitermales asociadas, Catamarca. In: Zappettini, E.O. (Ed.), Recursos Minerales de la República Argentina. Instituto de Geología y Recursos Minerales SEGEMAR (Buenos Aires), Anales, vol. 35, pp. 1479–1492.

Rossello, E.A., 1980. Nuevo complejo volcánico Vicuña Pampa, Departamento Belén, Provincia de Catamarca. Asociación Geológica Argentina, Revista 35, 436–438.

Rossello, E.A., 2000. Controles estructurales del lineamiento Tucumán sobre el magmatismo neógeno y sus mineralizaciones asociadas del Distrito Farallón Negro (Catamarca, Argentina): una revisión. Academia Nacional de Ciencias Exactas, Físicas y Naturales. Anales 52, 183–208.

Rossello, E.A., in press. La caldera Vicuña Pampa (27°00′S–67°00′0, Catamarca, Argentina): implicancias geotectónicas y económicas. Asociación Geológica Argentina, Revista.

Rossello, E.A., Mozetic, M.E., 1999. Caracterización estructural y significado geotectónico de los depositos cretácicos continentales del centro-oeste Argentino. Boletim do 5° Simpósio sobre o Cretáceo do Brasil (Serra Negra, SP, Brazil), pp. 107–113.

Rossello, E.A., de Urreiztieta, M., Gapais, D., Le Corre, C., Cobbold, P.R., 1996a. La elipticidad del Bajo La Alumbrera y la caldera del Cerro Galán (Catamarca, Argentina): ¿Reflejo de la deformación Andina? Asociación Geológica Argentina. Revista 51, 193–200.

Rossello, E.A., Mozetic, M.E., Cobbold, P.R., de Urreiztieta, M., Gapais, D., 1996b. El espolón Umango-Maz y la conjugacion sintaxial de los lineamientos Tucumán y Valle Fértil (La Rioja, Argentina). 13° Congreso Geológico Argentino-3° Congreso de Hidrocarburos (Buenos Aires, Argentina). Actas 2, 187–194.

Rossello, E.A., Mozetic, M.E., Cobbold, P.R., de Urreiztieta, M., Gapais, D., López-Gamundí, O., 1996c. The Valle Fértil flower structure and its relationships with the Precordillera and Pampean ranges, (30–32°S, Argentina). Third International Symposium on Andean Geodynamics, St. Malo, France, Extended Abstracts Volume, 481–484.

Routhier, P., 1980. Où sont les métaux de l'avenir? Mémoires du BRGM 105. 410 pp.

Salfity, J.A., 1985. Lineamientos transversales al rumbo andino en el noroeste Argentino. IV Congreso Geológico Chileno. Antofagasta, Chile, Part 2, pp. 119–137.

Salleb, A., 2003. Recherche de motifs fréquents pour l'extraction de règles d'association et de caractérisation. PhD Thesis, Orléans University, Orléans, France. 195 pp.

Salleb, A., Vrain, C., 2000. An application of association rule discovery to Geographic Information Systems. 4th European Conference on Principles and Practice of Knowledge Discovery in Databases (PKDD 2000), September 2000, Lyon, France, LNAI 1910Springer-Verlag, Berlin, Germany, pp. 613–618.

Sasso, A.M., Clark, A.H., 1998. The Farallón Negro Group, Northwest Argentina: magmatic, hydrothermal and tectonic evolution and implications for Cu–Au metallogeny in the Andean back-arc. Society of Economic Geologists Newsletter 34 (1), 8–18.

Somoza, R., 1998. Updated Nazca (Farallon)-South America relative motions during the last 40 My: implications for mountain building in the Central Andean region. Journal of South American Earth Sciences 11, 211–215.

Spaccapietra, S., Parent, C., Vangenot, C., 2000. GIS databases: from multiscale to multirepresentation. Abstraction, reformulation, and approximation, In: Choueiry, B.Y. and Walsh, T. (Eds.), LNAI 1864, Springer, 200 (Proceedings 4th International Symposium, SARA-2000, Horseshoe Bay, Texas, USA, July 26–29, 2000).

Sillitoe, R.H., 1997. Characteristics and controls of the largest porphyry copper–gold and epithermal gold deposits in the circum-Pacific region. Australian Journal of Earth Sciences 44, 373–388.

Toselli, A.J., 1996. Volcanismo andino. In: Aceñolaza, F.G., Miller, H., Toselli, A.J. (Eds.), Geología del Sistema de Famatina, Münchner Geologische Heste, vol. A25, pp. 295–296.

Tosdal, R.M., Richards, J.P., 2001. Magmatic and structural controls on the development of porphyry Cu ± Mo ± Au deposits. In: Richards, J.P., Tosdal, R.M. (Eds.), Structural Controls on Ore Genesis, Reviews in Economic Geology, vol. 14, pp. 157–180.

Turner, J.C., 1971. Carta Geológico-Económica de la República Argentina, Hoja 15d (Famatina), escala 1:200.000. Dirección General de Minas y Geología de Argentina, Buenos Aires.

Whitman, D., Isacks, B., Kay, S., 1996. Lithospheric structure and along-strike segmentation of the Central Andean Plateau: seismic Q, magmatism, flexure, topography and tectonics. Tectonophysics 259, 29–40.

Wyborn, L.A.I., Gallagher, R., Jagodzinski, E.A., 1994. A conceptual approach to metallogenic modelling using GIS: examples from the Pine Creek inlier. Proceedings of the Symposium on Australian Research in Ore Genesis, Australian Mineral Foundation, Adelaide, pp. 15.1–15.5.